PHYSICAL REVIEW D **87,** 033006 (2013)

Lepton flavor at the electroweak scale: A complete A_4 model

Martin Holthausen,[1,*] Manfred Lindner,[1,†] and Michael A. Schmidt[2,‡]

[1]*Max-Planck Institut für Kernphysik, Saupfercheckweg 1, 69117 Heidelberg, Germany*

[2]*School of Physics, ARC Centre of Excellence for Particle Physics at the Terascale, The University of Melbourne, Victoria 3010, Australia*

(Received 19 December 2012; published 19 February 2013)

Apparent regularities in fermion masses and mixings are often associated with physics at a high flavor scale, especially in the context of discrete flavor symmetries. One of the main reasons for that is that the correct vacuum alignment requires usually some high scale mechanism to be phenomenologically acceptable. Contrary to this expectation, we present in this paper a renormalizable radiative neutrino mass model with an A_4 flavor symmetry in the lepton sector, which is broken at the electroweak scale. For that we use a novel way to achieve the vacuum expectation value alignment via an extended symmetry in the flavon potential proposed before by two of the authors. We discuss various phenomenological consequences for the lepton sector and show how the remnants of the flavor symmetry suppress large lepton flavor violating processes. The model naturally includes a dark matter candidate, whose phenomenology we outline. Finally, we sketch possible extensions to the quark sector and discuss its implications for the LHC, especially how an enhanced diphoton rate for the resonance at 125 GeV can be explained within this model.

DOI: 10.1103/PhysRevD.87.033006 PACS numbers: 14.60.Pq, 14.60.St, 11.30.Hv, 12.15.Ff

I. INTRODUCTION

Much progress has been achieved in the field of particle physics during the last year. First, the last missing mixing angle θ_{13} of the Standard Model (SM) with massive neutrinos has been measured [1] to be 8° after first hints in 2011 [2] and recently an excess consistent with a SM Higgs has been observed at $126.0 \pm 0.4(\text{stat}) \pm 0.4(\text{sys})$ GeV by ATLAS [3,4] and at $125.8 \pm 0.4(\text{stat}) \pm 0.4(\text{sys})$ GeV by CMS [5,6].

Let us first discuss the implications of the large mixing angle θ_{13}. Much of the work in the neutrino sector has been aimed at explaining tiny values of θ_{13} as deviations from a tribimaximal (TBM) mixing structure using flavor symmetries, but this scenario is now implausible due to the sizeable value of θ_{13}.[1] So maybe there exists no symmetry that is connected to the regularities in the fermion parameters. It could rather be that mixing angles are determined at a high scale from some (quasi)random mechanism. Indeed if one randomly draws unitary 3×3 matrices with a probability measure given by the Haar measure of U(3), i.e., the unique measure that is invariant under a change of basis for the three generations, one finds a probability of 44% for nature to have taken a more "unusual" choice [9]. This cannot be interpreted, however, as an indication in favor of anarchy [10,11], as the sample (three mixing angles and one mass ratio) is clearly too small to reconstruct the probability measure to any degree of certainty [12]. The only statement one can make is that the (very limited) data cannot rule out the anarchy hypothesis. For any values of the mixing angles one can always find a flavor model that is in better agreement with the data.[2]

Another option is that flavor symmetries are realized in a different way. One route is to think of solutions that do not predict TBM. Such models are usually implemented at high scales and give precise predictions for the leptonic mixing angles in the experimentally allowed regions. These models might then be falsified in the same way that the models that give tribimaximal mixing have been ruled out, i.e., by a further refinement of the experimental determination of these angles. This seems to be the only fruitful direction for models that explain flavor at high energy scales such as the seesaw or grand unified theory scale, because mixing angles are generically the only experimentally testable predictions of such models. An example are models based on $\Delta(96)$ [14–16].

An interesting question is if flavor symmetries could even be realized at low scales [17–28]. If this is viable then such models can be tested by additional observables. Such observables typically include rare lepton flavor violating (LFV) decays of leptons and mesons and—ideally—a direct experimental access to the very fields that mediate the flavor symmetry breaking. Typically such models will feature extended Higgs sectors but will not uniquely determine the mixing angles; they will, however, rather give relations among the deviations from patterns such as tribimaximal mixing.

In this work we implement a model based on a flavor symmetry at the electroweak scale and show that it leads to

*martin.holthausen@mpi-hd.mpg.de
†lindner@mpi-hd.mpg.de
‡michael.schmidt@unimelb.edu.au

[1]See also the recent global fits to neutrino oscillations [7,8].

[2]This can be done without increasing the degree of complexity of the model [13].

additional phenomenological effects that will become testable in the future.

Many authors have noted that quite generic corrections in the neutrino sector within models based on the symmetry group A_4 [17,29] may lead to corrections to the leptonic mixing angles that are in agreement with the experimental data [30]. It should be noted, however, that all such models need to break the symmetry group in a particular way to different subgroups in the charged lepton and neutrino sectors, a vacuum configuration that cannot be obtained from a straightforward minimization of the potential but something that rather needs a special dynamical mechanism to achieve it. The two most commonly used mechanisms are either based on (i) continuous R symmetries in supersymmetry or (ii) extra dimensions. The supersymmetric models only work in the limit where the supersymmetry breaking scale is below the scale of flavor symmetry breaking and the scale of flavor symmetry breaking is thus unobservabely high. The only experimentally verifiable prediction of such models seem to be correlations in the deviations from TBM, e.g., the trimaximal mixing pattern that predicts $a \approx -\frac{1}{2} r \cos\delta$ and $s \approx 0$ where [31]

$$\begin{aligned} \sin\theta_{13} &= \frac{r}{\sqrt{2}}, \\ \sin\theta_{12} &= \frac{1}{\sqrt{3}}(1+s), \\ \sin\theta_{23} &= \frac{1}{\sqrt{2}}(1+a). \end{aligned} \tag{1.1}$$

As these models tend to be quite baroque, since they involve a large number of driving fields etc., this one prediction seems to be a rather poor showing compared to the model building effort involved. The second possibility using extra dimensions is possible, but we here want to focus on nonsupersymmetric models in four dimensions, a possibility that seems to be favored by the experimental data.

In an earlier work [32], two of us (M. H. and M. S.) have studied a possibility to obtain the vacuum alignment that seems to be quite close to the general spirit of discrete flavor model building: to get a predictive model one needs to have unbroken discrete remnant symmetries in the neutrino and charged lepton sectors that do not commute with each other. The way this is usually realized is that symmetries, particle content, and vacuum structure are selected such that these remnant symmetries are realized as accidental symmetries of the leading order mass matrices that are broken at next-to-leading order. The idea of Ref. [32], following earlier work by Babu and Gabriel [33], was to have an extended flavor group G and a particle content such that an accidental symmetry $G \times A_4$ arises at the renormalizable level in the scalar potential that allows for the desired vacuum configuration. More precisely, the scalars χ_i breaking the extended flavor group G in the charged lepton sector transform under the A_4 only, while the scalars ϕ_i breaking the extended flavor group G transform under the full group G. The symmetry is chosen such that the scalar potential does not contain operators with nontrivial contractions of χ_i with ϕ_i, i.e., there are only contractions of the form $(\chi_i\chi_j)_{\underline{\mathbf{1}}_1}(\phi_i\phi_j)_{\underline{\mathbf{1}}_1}$. The smallest symmetry group that realizes such a structure for A_4 is $G = Q_8 \rtimes A_4$ and since the symmetry breaking does not need any special additional ingredient, there is no immediate theoretical obstacle to have the flavor symmetry breaking scale at the electroweak scale.

In this work we therefore implement the model in Ref. [32] at the electroweak scale. The outline of the paper is as follows: We introduce the model and the exact symmetry breaking pattern in Sec. II. Without the introduction of any additional symmetries, we show in Sec. III that neutrino masses are generated at one-loop level and that the neutrino mass matrix is determined by five physical parameters. We discuss the predictions for neutrino oscillation observables that follow from this structure. In Sec. IV, we discuss constraints from lepton-flavor violating rare decays. In Sec. V, we show that the model contains a dark matter candidate and discuss its phenomenology. Three simple possible extensions to the quark sector are discussed in Sec. VI. Finally, in Sec. VII we discuss the implications of direct collider searches and the recent observation of a Higgs-like boson at 125 GeV and then we conclude in Sec. VIII.

II. MODEL AND SYMMETRY BREAKING

We utilize the symmetry $Q_8 \rtimes A_4$ introduced in Ref. [32], which allows for natural vacuum alignment, and implement a model describing the lepton sector at the electroweak scale. Hence, we promote the flavon fields of Ref. [32] that couple to the charged lepton sector to electroweak (EW) Higgs doublets. The particle content of the lepton sector is given in Table I. The vacuum configuration

$$\begin{gathered} \langle\chi_i\rangle = \begin{pmatrix} 0 \\ \frac{v}{\sqrt{6}} \end{pmatrix}, \qquad \langle\phi_1\rangle = \frac{1}{\sqrt{2}}(a, a, b, -b)^T, \\ \langle\phi_2\rangle = \frac{1}{\sqrt{2}}(c, c, d, -d)^T \end{gathered} \tag{2.1}$$

TABLE I. Particle content of the minimal model that realizes flavor symmetry breaking at the electroweak scale. The flavon χ contains the Higgs field and ties the electroweak to the flavor breaking scale. The scalars η_i and fermionic multiplet S are needed for one-loop generation of neutrino masses.

	L	e^c	μ^c	τ^c	χ	ϕ_1	ϕ_2	S	η_1	η_2	η_3
$Q_8 \rtimes A_4$	$\underline{\mathbf{3}}_1$	$\underline{\mathbf{1}}_1$	$\underline{\mathbf{1}}_2$	$\underline{\mathbf{1}}_3$	$\underline{\mathbf{3}}_1$	$\underline{\mathbf{4}}_1$	$\underline{\mathbf{4}}_1$	$\underline{\mathbf{3}}_2$	$\underline{\mathbf{3}}_5$	$\underline{\mathbf{3}}_4$	$\underline{\mathbf{3}}_5$
Z_4	i	$-$i	$-$i	$-$i	1	1	-1	-1	i	i	$-$i
$\mathrm{SU}(2)_L$	2	1	1	1	2	1	1	1	2	2	2
$\mathrm{U}(1)_Y$	$-1/2$	1	1	1	1/2	0	0	0	1/2	1/2	1/2

can be naturally obtained from the most general scalar potential following the discussion in Ref. [32]. As the discussion is very similar to the one given there, we relegate it to Appendix A 1, where also the scalar mass spectrum is discussed. However, let us briefly recall the salient features of the vacuum expectation value (VEV) configuration (2.1): the scalar singlets ϕ_1 and ϕ_2 break the symmetry group to the subgroup $\langle S|S^2 = E\rangle \cong Z_2$ and the EW doublets χ break the discrete symmetry group down to the subgroup $\langle T|T^3 = E\rangle \cong Z_3$, while simultaneously breaking the electroweak gauge group $\mathrm{SU}(2)_L \times \mathrm{U}(1)_Y$ down to the electromagnetic $\mathrm{U}(1)_{\mathrm{em}}$. The normalization is chosen such that $\sum_i v_i^2 = v^2 = (\sqrt{2}G_F)^{-1} = (246\,\mathrm{GeV})^2$, in accordance with our earlier definition. Because of the unbroken Z_3 symmetry in the charged lepton sector, it is useful to go to a basis [17,22–24]

$$\begin{aligned}(H, \varphi', \varphi'')^T &= \Omega_T^\dagger \chi \sim (1, \omega^2, \omega),\\ (L_e, L_\mu, L_\tau)^T &= \Omega_T^\dagger L \sim (1, \omega^2, \omega),\end{aligned} \tag{2.2}$$

where this symmetry is represented diagonally and Ω_T is defined by

$$\Omega_T \equiv \frac{1}{\sqrt{3}}\begin{pmatrix}1 & 1 & 1\\ 1 & \omega^2 & \omega\\ 1 & \omega & \omega^2\end{pmatrix}. \tag{2.3}$$

We have indicated the transformation properties under the unbroken subgroup $\langle T\rangle \cong Z_3$ under which (e^c, μ^c, τ^c) transform as $(1, \omega, \omega^2)$. This has been denoted flavor triality in Ref. [22]. In this basis the vacuum configuration (2.1) implies that only the field H acquires a VEV $\langle H\rangle = (0, v/\sqrt{2})^T$, while φ' and φ'' are inert doublets (and thus do not obtain a VEV). The potential for the electroweak doublets χ is given by

$$\begin{aligned}V_\chi(\chi) = \mu_3^2 \chi^\dagger\chi + \sum_{r=\underline{\mathbf{1}}_{1,2},\underline{\mathbf{3}}_{1S,1A}} \lambda_{\chi r}(\chi^\dagger\chi)_r(\chi^\dagger\chi)_{r^*}\\ + \lambda_{\chi A}\mathrm{Im}\Big[(\chi^\dagger\chi)_{\underline{\mathbf{3}}_{1S}}(\chi^\dagger\chi)_{\underline{\mathbf{3}}_{1A}}\Big],\end{aligned} \tag{2.4}$$

and after symmetry breaking the nine physical scalars contained in χ arrange themselves in the following multiplets under the remnant $\mathrm{U}(1) \times Z_3$ symmetry. There is one real scalar $h = \sqrt{2}\mathrm{Re}H^0$ with mass

$$m_h^2 = \frac{2}{9}\Big(3\lambda_{\chi 1_1} + \sqrt{3}\lambda_{\chi 3_{1,S}}\Big)v^2 \tag{2.5}$$

that plays the role of the Standard Model Higgs boson. Note that since this scalar is a complete singlet under all remnant symmetries, it can in principle mix with components of ϕ_1 and ϕ_2 that transform in the same way. This is discussed in detail in Eq. (A9), and in the following we will for the most part assume the mixing to be small enough to treat h as a mass eigenstate.

The next 4 degrees of freedom are in the charged scalars φ'^+ and φ''^+ that transform as $(1, \omega^2)$ and $(1, \omega)$ under $\mathrm{U}(1) \times Z_3$, respectively, and have the masses

$$\begin{aligned}m_{\varphi'^+}^2 &= \frac{v^2}{12}\Big(-2\sqrt{3}\lambda_{\chi 3_{1,S}} - \lambda_{\chi A}\Big),\\ m_{\varphi''^+}^2 &= \frac{v^2}{12}\Big(-2\sqrt{3}\lambda_{\chi 3_{1,S}} + \lambda_{\chi A}\Big).\end{aligned} \tag{2.6}$$

The final four real scalars sit in the two complex neutral scalars φ'^0 and φ''^{0*}, that both transform as $(0, \omega^2)$ and the mass eigenstates are given by the neutral scalars

$$\begin{pmatrix}\Phi_1\\ \Phi_2\end{pmatrix} = U_\varphi\begin{pmatrix}\varphi'^0\\ \varphi''^{0*}\end{pmatrix} \equiv \begin{pmatrix}\cos\alpha & \sin\alpha\\ -\sin\alpha & \cos\alpha\end{pmatrix}\begin{pmatrix}\varphi'^0\\ \varphi''^{0*}\end{pmatrix}. \tag{2.7}$$

The mixing angle α and their masses may be written as

$$\tan 2\alpha = \frac{6\lambda_{\chi 1_2} + \sqrt{3}\Big(3\lambda_{\chi 3_{1,A}} + \lambda_{\chi 3_{1,S}}\Big)}{6\lambda_{\chi A};}, \tag{2.8}$$

$$\begin{aligned}m_{\Phi_1}^2 + m_{\Phi_2}^2 = -2\tan(2\alpha)(m_{\varphi''^+}^2 - m_{\varphi'^+}^2)\\ + m_{\varphi''^+}^2 + m_{\varphi'^+}^2 - \frac{v^2\lambda_{\chi 3_{1,A}}}{\sqrt{3}},\end{aligned} \tag{2.9}$$

$$m_{\Phi_1}^2 - m_{\Phi_2}^2 = 2|\sec(2\alpha)||m_{\varphi''^+}^2 - m_{\varphi'^+}^2|. \tag{2.10}$$

The mass spectra for the other scalars can be found in Appendix A 2. Two comments are in order here: (i) in the potential (2.4) there is only one mass term for the three doublets. Using the minimization conditions, the mass term can be swapped for the Higgs VEV v and therefore (ii) all of the squared scalar masses are given as a product of dimensionless scalar couplings times v^2. The additional scalar masses may therefore not be arbitrarily large. Note that in usual multi-Higgs doublet models, each doublet has its own mass term and therefore there is always a decoupling limit where all non-SM particles are unobservably heavy. Such a setup is therefore directly testable at colliders, as we will study in Sec. VII. However, before discussing this, we show that the model accomplishes (i) the description of the (lepton) flavor structure in terms of a small number of parameters and (ii) the protection against bounds on new physics from flavor observables such as lepton flavor violating processes.

III. LEPTON FLAVOR STRUCTURE

In this section we discuss the one-loop generation of neutrino masses and phenomenological implications of the predicted flavor structure.

A. Lepton masses

The charged lepton sector is described by

$$-\mathcal{L}_e = y_e L\tilde{\chi}e^c + y_\mu L\tilde{\chi}\mu^c + y_\tau L\tilde{\chi}\tau^c + \mathrm{H.c.}, \tag{3.1}$$

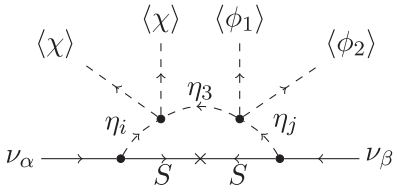

FIG. 1. Neutrino mass generation at one loop.

where $\tilde{\chi} = i\sigma_2\chi^*$ and here and in the following we do not specifically indicate the contractions if there is only one invariant that can be formed out of the particle content of the operator. In the physical basis of Eq. (2.2) this term reads

$$\begin{aligned} -\mathcal{L}_e = {} & \tilde{H}(y_e L_e e^c + y_\mu L_\mu \mu^c + y_\tau L_\tau \tau^c) \\ & + \tilde{\varphi}'(y_e L_\mu e^c + y_\mu L_\tau \mu^c + y_\tau L_e \tau^c) \\ & + \tilde{\varphi}''(y_e L_\tau e^c + y_\mu L_e \mu^c + y_\tau L_\mu \tau^c) + \text{H.c.}, \end{aligned} \tag{3.2}$$

and we thus see that H couples diagonally to leptons while φ' and φ'' do not. Note that here the mass terms are generated by dimension four Yukawa couplings and there is therefore no need for a complicated UV completion. The mass matrix is thus given by

$$M_E = \frac{v}{\sqrt{2}}\Omega_T^* \text{diag}(y_e, y_\mu, y_\tau), \tag{3.3}$$

with Ω_T given in Eq. (2.3). Neutrino masses are generated at one-loop level, through the interactions with the fermionic singlets S and the scalar doublets η, as shown in Fig. 1. The couplings of S are given by

$$\mathcal{L}_\nu = h_1 L \eta_1 S + h_2 L \eta_2 S + \sqrt{3} M_S S S + \text{H.c.} \tag{3.4}$$

The factor of $\sqrt{3}$ cancels a factor coming from the normalization of Clebsch-Gordon coefficients. In order to calculate the neutrino mass matrix, we have to determine the mass matrix of the neutral components of η_1, η_2, and η_3. To shorten the notation we define the doublet $\hat{\eta}_J$ to be the Jth component of the nine-component vector $\hat{\eta} = (\eta_1, \eta_2, \eta_3)$ and real scalar field $\hat{\eta}^0_k$ to be the kth component of $(\sqrt{2}\text{Re}\hat{\eta}^0, \sqrt{2}\text{Im}\hat{\eta}^0)$. Besides the direct mass terms

$$(M^2_{\eta^0})_{ij} = \frac{\partial^2 V^{(2)}_{\eta_i}}{\partial \hat{\eta}^0_i \partial \hat{\eta}^0_j} \quad \text{with} \quad V^{(2)}_{\eta_i} = \sum_{i=1,2,3} \sqrt{3}\, M_i^2 \eta_i^\dagger \eta_i, \tag{3.5}$$

there are couplings that give off-diagonal contributions

$$(\delta M^2_{\eta^0})_{ij} = \left\langle \frac{\partial^2 \delta V^{(2)}_{\eta_i}}{\partial \hat{\eta}^0_i \partial \hat{\eta}^0_j} \right\rangle \tag{3.6}$$

to the mass matrix. Such interactions are needed to generate neutrino masses and the relevant ones can be determined from symmetry considerations.[3] Any contribution to neutrino mass has to be proportional to

(i) M_S, which breaks the generalized lepton number $L \to e^{i\alpha}L$, $S \to e^{-i\alpha}S$,

(ii) either of the couplings λ_1 or λ_2, defined by[4]

$$\begin{aligned} V_{\eta,\chi} = {} & \lambda_1 (\chi^T \sigma_2 \vec{\sigma} \chi)_{\underline{\mathbf{1}}_1} (\eta_1^T \sigma_2 \vec{\sigma} \eta_3)^*_{\underline{\mathbf{1}}_1} \\ & + \lambda_2 e^{i\alpha_\lambda} (\chi^T \sigma_2 \vec{\sigma} \chi)_{\underline{\mathbf{3}}_1} (\eta_2^T \sigma_2 \vec{\sigma} \eta_3)^*_{\underline{\mathbf{3}}_1} + \text{H.c.}, \end{aligned} \tag{3.7}$$

which break the generalized lepton number $L \to e^{i\alpha}L$, $\eta_i \to e^{-i\alpha}\eta_i$,

(iii) and λ_3 or λ_4 defined by[5]

$$\begin{aligned} V_{\eta,\phi} = {} & \lambda_3 (\phi_1 \phi_2)_{\underline{\mathbf{1}}_1} (\eta_3^\dagger \eta_1)_{\underline{\mathbf{1}}_1} \\ & + \lambda_4 (\phi_1 \phi_2)_{\underline{\mathbf{3}}_1} (\eta_3^\dagger \eta_2)_{\underline{\mathbf{3}}_1} + \text{H.c.}, \end{aligned} \tag{3.8}$$

which couples to the Z_4-breaking VEV of ϕ_2.

The built-in multiple protection of the neutrino mass operator thus necessitates the large number of couplings involved in neutrino mass generation, and thus a large potential for suppression beyond the naive factor of $1/(16\pi^2)$ from the loop integral. For simplicity, we assume that the direct mass terms M_i dominate over all other contributions; this is in fact a necessary condition to have a predictive theory of flavor. Hence, we can approximate the propagator as

$$\begin{aligned} & [k^2 - (M^2_{\eta^0} + \delta M^2_{\eta^0})]^{-1} \\ & \quad = (k^2 - M^2_{\eta^0})^{-1} + (k^2 - M^2_{\eta^0})^{-1} \delta M^2_{\eta^0} (k^2 - M^2_{\eta^0})^{-1}, \end{aligned} \tag{3.9}$$

where $M^2_{\eta^0}$ is diagonal, and treat the mixing between the different components of η_i by mass insertions $\delta M^2_{\eta^0}$. The evaluation of the one-loop diagram leads to

$$\begin{aligned} (M_\nu)_{\alpha\beta} = {} & \sum_{i=1}^{3} \sum_{I,J,M=1}^{18} h_{\alpha i I} h_{\beta i J} M_S (\delta M^2_{\eta^0})_{IM} (\delta M^2_{\eta^0})_{MJ} \\ & \times I((M^2_{\eta^0})^{\frac{1}{2}}_{II}, (M^2_{\eta^0})^{\frac{1}{2}}_{JJ}, (M^2_{\eta^0})^{\frac{1}{2}}_{MM}, M_S), \end{aligned} \tag{3.10}$$

where the Yukawa couplings h_{ikJ} depend on the two couplings $h_{1,2}$ given in Eq. (3.4) via

[3]The complete expression for $\delta V^{(2)}_{\eta_i}$ can be found in Eq. (A10). Here, we only present the parts that are relevant for neutrino masses.

[4]We can set a number of complex parameters real by phase redefinitions. We set y_e, y_μ, y_τ, h_1, h_2, M_S, λ_1, λ_3, λ_4 real by rotating ℓ^c, L, η_2, S, χ, η_1, η_3, respectively, and display the phase of λ_2 explicitly.

[5]The contractions $(\chi^T \sigma_2 \vec{\sigma} \chi)_{\underline{\mathbf{1}}_{2,3}}$ vanish in the vacuum given in Eq. (2.1) and thus do not contribute to the masses here, because the Z_3 symmetry generated by T is conserved by $\langle\chi\rangle$.

$$h_{\alpha k J} = \frac{\partial \mathcal{L}_\nu}{\partial L_\alpha \partial S_k \partial \hat{\eta}_J}, \tag{3.11}$$

and the loop integral is given by[6]

$$I(m_1, m_2, m_3, m_4) = -\frac{1}{16\pi^2} \sum_i \frac{m_i^2 \log\left(\frac{m_i^2}{\mu^2}\right)}{\Pi_{k\neq i}(m_i^2 - m_k^2)}. \tag{3.12}$$

Evaluation of the sums leads to the following flavor structure of the neutrino mass matrix:

$$M_\nu = \begin{pmatrix} \hat{a} & \hat{e}e^{i\alpha_\lambda} & \hat{e}e^{i\alpha_\lambda} \\ . & \hat{a} + \hat{b}e^{i\alpha_\lambda} & \hat{d} + \hat{e}e^{i\alpha_\lambda} \\ . & . & \hat{a} \end{pmatrix}, \tag{3.13}$$

where the four real coefficients are given by

$$\hat{a} = \frac{1}{36\sqrt{3}} h_1^2 \lambda_3 \lambda_1 v^2 (ac + bd) M_S I(M_1, M_1, M_3, M_S), \tag{3.14a}$$

$$\hat{d} = \frac{1}{72\sqrt{3}} h_1 h_2 \lambda_4 \lambda_1 v^2 (bc - ad) M_S I(M_1, M_2, M_3, M_S), \tag{3.14b}$$

$$\hat{b} = \frac{1}{108} h_2^2 \lambda_4 \lambda_2 v^2 (bc - ad) M_S I(M_2, M_2, M_3, M_S), \tag{3.14c}$$

$$\hat{e} = \frac{1}{216} h_1 h_2 \lambda_3 \lambda_2 v^2 (ac + bd) M_S I(M_1, M_2, M_3, M_S). \tag{3.14d}$$

Hence, neutrino masses are suppressed by one insertion of the EW breaking VEV $\lambda_1 \langle \chi^2 \rangle / M_0^2$, with M_0 being the largest mass of the particles in the loop $M_0 \sim \max_{i=1,2,3,S} M_i$, and one mass insertion of the flavor breaking VEV $\lambda_2 \langle \phi_1 \phi_2 \rangle / M_0^2$. A phenomenologically viable neutrino mass scale is obtained for e.g., $M_0 \sim \mathcal{O}(\text{TeV})$, $\langle \chi \rangle$, $\langle \phi_i \rangle \sim \mathcal{O}(100\ \text{GeV})$, and h_i, $\lambda_i \sim \mathcal{O}(0.01\text{–}0.1)$. The next-to-leading order corrections are suppressed by $\lambda_1 \langle \chi^2 \rangle / M_0^2$ or $\lambda_2 \langle \phi_1 \phi_2 \rangle / M_0^2$, which amounts to an $\mathcal{O}(0.0001\text{–}0.001)$ correction for our typical values and can be neglected to a good approximation.

The neutrino mass elements correspond to the following operators:

(i) $\hat{a}$: $(L^T \sigma_2 \vec{\sigma} L)_{\underline{1}_1} (\chi^T \tau_2 \vec{\tau} \chi)_{\underline{1}_1} (\phi_1 \phi_2)_{\underline{1}_1}$,
(ii) $\hat{d}$: $(L^T \sigma_2 \vec{\sigma} L)_{\underline{3}_1} (\chi^T \sigma_2 \vec{\sigma} \chi)_{\underline{1}_1} (\phi_1 \phi_2)_{\underline{3}_1}$,
(iii) $\hat{e}$: $(L^T \sigma_2 \vec{\sigma} L)_{\underline{3}_1} (\chi^T \sigma_2 \vec{\sigma} \chi)_{\underline{3}_1} (\phi_1 \phi_2)_{\underline{1}_1}$,
(iv) $\hat{b}$: $\sum_i \omega^{i-1} (L^T \sigma_2 \vec{\sigma} L)_{\underline{1}_i} [(\chi^T \sigma_2 \vec{\sigma} \chi)_{\underline{3}_1} (\phi_1 \phi_2)_{\underline{3}_1}]_{\underline{1}_i^*}$.

The fact that only the combination shown in the last line contributes to neutrino masses is due to the UV completion presented here. In a general theory one might have all operators present, thereby reducing the predictability of the theory.

B. Phenomenological implications

As the neutrino mass matrix is described by five physical real parameters, there are four predictions in the lepton sector at leading order. They can easily be read off from Eq. (3.13) in terms of matrix elements, but the expressions in terms of mixing parameters are nontrivial. In the flavor basis, where the charged lepton mass matrix is diagonal, the neutrino mass matrix is given by

$$M_\nu^{\text{fl}} = \begin{pmatrix} \hat{a} + \frac{2\hat{d}}{3} + \left(2\hat{e} + \frac{\hat{b}}{3}\right)e^{i\alpha_\lambda} & -\frac{\hat{d}}{3} + \frac{\hat{b}}{3} e^{i\alpha_\lambda} \omega^2 & -\frac{\hat{d}}{3} + \frac{\hat{b}}{3} e^{i\alpha_\lambda} \omega \\ . & \frac{2\hat{d}}{3} + \frac{\hat{b}}{3} e^{i\alpha_\lambda} \omega & \hat{a} - \frac{\hat{d}}{3} + \left(\frac{\hat{b}}{3} - \hat{e}\right)e^{i\alpha_\lambda} \\ . & . & \frac{2\hat{d}}{3} + \frac{\hat{b}}{3} e^{i\alpha_\lambda} \omega^2 \end{pmatrix}, \tag{3.15}$$

and it is instructive to look at the neutrino mass matrix in the tribimaximal basis $M_\nu^{\text{tbm}} = U_{\text{HPS}}^T M_\nu^{\text{fl}} U_{\text{HPS}}$, i.e.,

$$M_\nu^{\text{tbm}} = \begin{pmatrix} \hat{a} + \hat{d} + \left(\frac{\hat{b}}{2} + \hat{e}\right)e^{i\alpha_\lambda} & -\sqrt{2}\hat{e}e^{i\alpha_\lambda} & -i\frac{\hat{b}}{2} e^{i\alpha_\lambda} \\ . & \hat{a} & 0 \\ . & . & -\hat{a} + \hat{d} + \left(\hat{e} - \frac{\hat{b}}{2}\right)e^{i\alpha_\lambda} \end{pmatrix}. \tag{3.16}$$

We will first discuss limiting cases analytically and then perform a numerical analysis of the general neutrino mass matrix. In the limit of $|\lambda_2| v^2 \to 0$, both $\hat{b}$ and $\hat{e}$ vanish and we obtain tribimaximal mixing

[6]Note that the renormalization scale μ drops out of the sum; it is displayed here to make the symmetric structure of the expression explicit, while keeping the argument of the logarithm dimensionless.

$$U_{\rm HPS} \equiv \Omega_T^\dagger \Omega_U = \begin{pmatrix} \sqrt{\frac{2}{3}} & \frac{1}{\sqrt{3}} & 0 \\ -\frac{1}{\sqrt{6}} & \frac{1}{\sqrt{3}} & \frac{1}{\sqrt{2}} \\ -\frac{1}{\sqrt{6}} & \frac{1}{\sqrt{3}} & -\frac{1}{\sqrt{2}} \end{pmatrix} \quad \text{with} \quad \Omega_U = \begin{pmatrix} 0 & 1 & 0 \\ \frac{1}{\sqrt{2}} & 0 & -\frac{i}{\sqrt{2}} \\ \frac{1}{\sqrt{2}} & 0 & \frac{i}{\sqrt{2}} \end{pmatrix}. \tag{3.17}$$

From Eq. (3.16) we can read off that switching on $\hat{e} \neq 0$ while keeping $\hat{b} = 0$ results in a correction to the Pontecorvo-Maki-Nakagawa-Sakata (PMNS) matrix of the form $U = U_{\rm HPS} U_{12}(\tilde{\theta}_{12}) P$ with $U_{12}(\tilde{\theta}_{12})$ denoting the unitary matrix

$$U_{12}(\tilde{\theta}) = \begin{pmatrix} c_{12} & -s_{12} e^{-i\delta_{12}} & \\ s_{12} e^{i\delta_{12}} & c_{12} & \\ & & 1 \end{pmatrix}, \tag{3.18}$$

with $c_{12} = \cos\tilde{\theta}_{12}$, $s_{12} = \sin\tilde{\theta}_{12}$, and P being an arbitrary phase matrix. In the standard parametrization of the PMNS matrix [34] with the 1–2 rotation to the right, this 1–2 correction only affects the solar angle, while maintaining the predictions of a maximal atmospheric and vanishing reactor angle. Since large corrections to this angle are not allowed, in the phenomenologically acceptable parameter space the relations $\hat{e} \ll \hat{b}, \hat{a}, \hat{d}$ should hold.

On the other hand, if we take $\hat{b} \neq 0$ while $\hat{e} = 0$, we see from Eq. (3.16) that this requires a 1–3 correction $U = U_{\rm HPS} U_{13}(\tilde{\theta}_{13}) P$, where $U_{13}(\tilde{\theta}_{13})$, analogous to $U_{12}(\tilde{\theta}_{12})$, denotes a complex rotation in the 1–3 plane. This correction is of the trimaximal mixing [30,31,35–39] form, which can perturb TBM back into agreement with experiment. The effect of the various deviations from TBM is illustrated in Fig. 2.

To gain an analytical understanding of how the additional parameters affect the mixing angles, we can perform a perturbative analysis in the limit of small $\hat{e}$ and therefore small $|\sin^2\theta_{12} - \frac{1}{3}|$. The PMNS matrix can be described by $U_{\rm HPS} U_{13}(\tilde{\theta}_{13}) U_{12}(\tilde{\theta}_{12}) P$, where $\tilde{\theta}_{12}$ and $\tilde{\theta}_{13}$ are small in the phenomenologically interesting region and the Majorana phases are given by $P = \mathrm{diag}(e^{i\alpha_1/2}, 1, e^{i\alpha_3/2})$. Hence, we can permute the matrices U_{12} and U_{13} and we define $r_{1i} = \sin\tilde{\theta}_{1i}\cos\tilde{\delta}_{1i}$ and $t_{1i} = \tan\tilde{\delta}_{1i}$, which evaluate to

$$r_{13} = \frac{\hat{b}\sin\alpha_\lambda}{4\hat{a} + 2\hat{b}\cos\alpha_\lambda}, \qquad t_{13} = \frac{2\hat{a}\cos\alpha_\lambda + \hat{b}}{2\hat{d}\sin\alpha_\lambda}, \tag{3.19a}$$

$$r_{12} = \frac{\sqrt{2}\hat{d}\,\hat{e}\sin\alpha_\lambda}{\Delta m^2_{21,0}}, \qquad t_{12} = \frac{2(2\hat{a} + \hat{d})\cos\alpha_\lambda + \hat{b}}{2\hat{d}\sin\alpha_\lambda}, \tag{3.19b}$$

where $\Delta m^2_{21,0}$ is the leading order solar mass squared difference, i.e., neglecting the small corrections of r_{13} and $\hat{e}$. The phases of the matrix P are given by

$$\tan\alpha_1 = \frac{2\hat{b}r_{13}\cos\alpha_\lambda - \sin\alpha_\lambda(2\hat{b}r_{13}t_{13} + \hat{b} + 2\hat{e})}{2(\hat{a} + \hat{b}r_{13}\sin\alpha_\lambda + \hat{d}) + \cos\alpha_\lambda(2\hat{b}r_{13}t_{13} + \hat{b} + 2\hat{e})}, \tag{3.20a}$$

$$\tan\alpha_2 = \frac{\sin\alpha_\lambda(\hat{b}(2r_{13}t_{13} - 1) + 2\hat{e}) + 2\hat{b}r_{13}\cos\alpha_\lambda}{2(\hat{a} + \hat{b}r_{13}\sin\alpha_\lambda - \hat{d}) + \cos\alpha_\lambda(-2\hat{b}r_{13}t_{13} + \hat{b} - 2\hat{e})}. \tag{3.20b}$$

Similar to Ref. [31], we can parametrize the leptonic mixing matrix in terms of deviations from the tribimaximal mixing angles as defined in Eq. (1.1). The Dirac CP phase δ_{CP} is undefined in the tribimaximal mixing limit and we leave it free and do not expand in it. Besides the contributions of $\alpha_{1,3}$ to the Majorana phases $\varphi_{1,2}$ in the standard parametrization, there are also small corrections $\delta\varphi_{1,2}$ from the matrices $U_{12}(\tilde{\theta}_{12})$ and $U_{13}(\tilde{\theta}_{13})$ resulting in

$$\varphi_1 = \alpha_1 - \alpha_3 + \delta\varphi_1, \quad \text{and} \quad \varphi_2 = \pi - \alpha_3 + \delta\varphi_2. \tag{3.21}$$

This expansion leads to the following form of the PMNS matrix:

$$U = \begin{pmatrix} \frac{s + i\delta\varphi_1 - 2}{\sqrt{6}} & \frac{2i(s+1) + \delta\varphi_2}{2\sqrt{3}} & -\frac{e^{-i\delta} r}{\sqrt{2}} \\ \frac{2(-a + e^{i\delta} r + s + 1) - i\delta\varphi_1}{2\sqrt{6}} & \frac{\delta\varphi_2 - i(2a + e^{i\delta} r + s - 2)}{2\sqrt{3}} & -\frac{a+1}{\sqrt{2}} \\ \frac{2(a - e^{i\delta} r + s + 1) - i\delta\varphi_1}{2\sqrt{6}} & \frac{i(2a + e^{i\delta} r - s + 2) + \delta\varphi_2}{2\sqrt{3}} & -\frac{a-1}{\sqrt{2}} \end{pmatrix} P. \tag{3.22}$$

Equating the expanded form of U to $U_{\rm HPS} U_{13}(\tilde{\theta}_{13}) U_{12}(\tilde{\theta}_{12}) P$ determines all free parameters s, r, a, δ, $\delta\varphi_1$, $\delta\varphi_2$ as well as some corrections to unphysical phases, which we suppressed for simplicity. The first order deviations from the mixing angles are

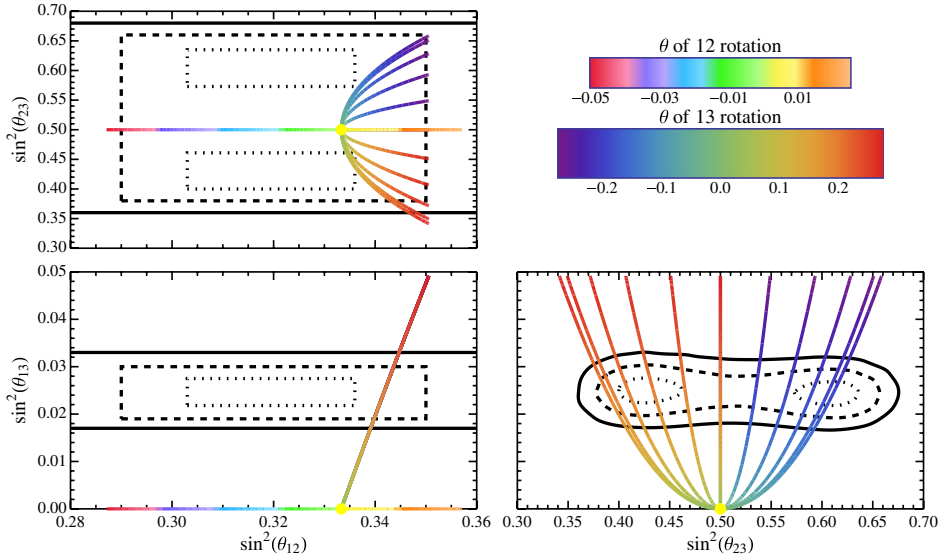

FIG. 2 (color online). The deviations from tribimaximal mixing of the form $U = U_{\mathrm{HPS}}U_{12}$ and $U = U_{\mathrm{HPS}}U_{13}$ generated by the angle θ defined in Eq. (3.18). The yellow point represents TBM, the continuous lines give the deviations from TBM with the angle θ given by the color codes in the top right corner for $\delta = \frac{n}{5}\frac{\pi}{2}$ for $n = 0, \ldots, 5$, where $n = 0$ is the outermost parabola etc. The 1, 2, and 3 sigma regions of a recent global fit [7] are indicated by dotted, dashed, and continuous contours, respectively.

$$s = -\sqrt{2}r_{12}t_{12}, \qquad r\cos\delta = -\frac{2r_{13}}{\sqrt{3}}, \qquad a = \frac{r_{13}}{\sqrt{3}}, \tag{3.23}$$

and the CP phases are given by

$$\tan\delta_{CP} = \tan\tilde{\delta}_{13}, \qquad \varphi_1 = \alpha_1 - \alpha_3 - 2\sqrt{2}r_{12}, \qquad \varphi_2 = \pi - \alpha_3 - 2\sqrt{2}r_{12}. \tag{3.24}$$

Following Ref. [31], we can derive a sum rule, which relates the deviations of the atmospheric mixing angle with the ones of the reactor mixing angle

$$a = -\frac{1}{2}r\cos\delta_{CP}. \tag{3.25}$$

The masses are determined by

$$\begin{aligned} m_1^2 &= \hat{a}^2 + \hat{b}(\hat{a} + \hat{d})\cos\alpha_\lambda + 2\hat{a}\,\hat{d} + \frac{\hat{b}^2}{4} + \hat{d}^2, \\ m_2^2 &= \hat{a}^2, \\ m_3^2 &= \hat{a}^2 + \hat{b}(\hat{a} - \hat{d})\cos\alpha_\lambda - 2\hat{a}\,\hat{d} + \frac{\hat{b}^2}{4} + \hat{d}^2, \end{aligned} \tag{3.26}$$

to leading order in the small mixings r_{13}, r_{12}, and the leading order ratio of mass squared differences is given by

$$\frac{\Delta m_{21}^2}{\Delta m_{32}^2} = \frac{4\hat{a}(2\hat{d} + \hat{b}\cos\alpha_\lambda) + 4\hat{d}(\hat{d} + \hat{b}\cos\alpha_\lambda) + \hat{b}^2}{4\hat{a}(2\hat{d} - \hat{b}\cos\alpha_\lambda) - 4\hat{d}(\hat{d} - \hat{b}\cos\alpha_\lambda) - \hat{b}^2}. \tag{3.27}$$

At next-to-leading order, m_1 and m_3 receive corrections

$$\delta m_1^2 = \hat{b}(2r_{13}(\hat{a} + \hat{d})\sin\alpha_\lambda + \hat{b}r_{13}t_{13} + \hat{e}) + 2(\hat{a} + \hat{d})\cos\alpha_\lambda(\hat{b}r_{13}t_{13} + \hat{e}), \tag{3.28a}$$

$$\delta m_3^2 = -\hat{b}(-2r_{13}(\hat{a} - \hat{d})\sin\alpha_\lambda + \hat{b}r_{13}t_{13} + \hat{e}) - 2(\hat{a} - \hat{d})\cos\alpha_\lambda(\hat{b}r_{13}t_{13} + \hat{e}). \tag{3.28b}$$

To illustrate our findings numerically, we have performed a numerical scan over the model's parameter space. We have randomly drawn values for the model parameters of order unity, assuming a Gaussian distribution with an expectation value of 1 and a variance of 0.5. The plots in Fig. 3 show the relation between the atmospheric mixing angle θ_{23} and the reactor angle θ_{13}. From the bottom two plots one can read off that $\hat{b}$ is of the same order as $\hat{a}$ and $\hat{d}$ for the experimentally measured θ_{13} while $\hat{e}$ has to be about 1 order of magnitude smaller. The color codings of the two top panels show the mixing parameters δ_{CP} and $\sin^2\theta_{12}$. Clearly, the model is predictive: if $\sin^2\theta_{23}$ is found to be close to the best fit point in the octant with $\sin^2\theta_{23} < 1/2$, the prediction for the CP phase is $\delta_{CP} = 0, 2\pi$ while for $\sin^2\theta_{23} > 1/2$ it is predicted to be $\delta_{CP} = \pi$. To establish the correlation with $\sin^2\theta_{12}$ shown in the top right panel, a precision determination of all the mixing angles is needed. In Fig. 4, as a consistency check of our analytical expressions, the atmospheric sum rule (3.25) is shown for the points obtained in the numerical

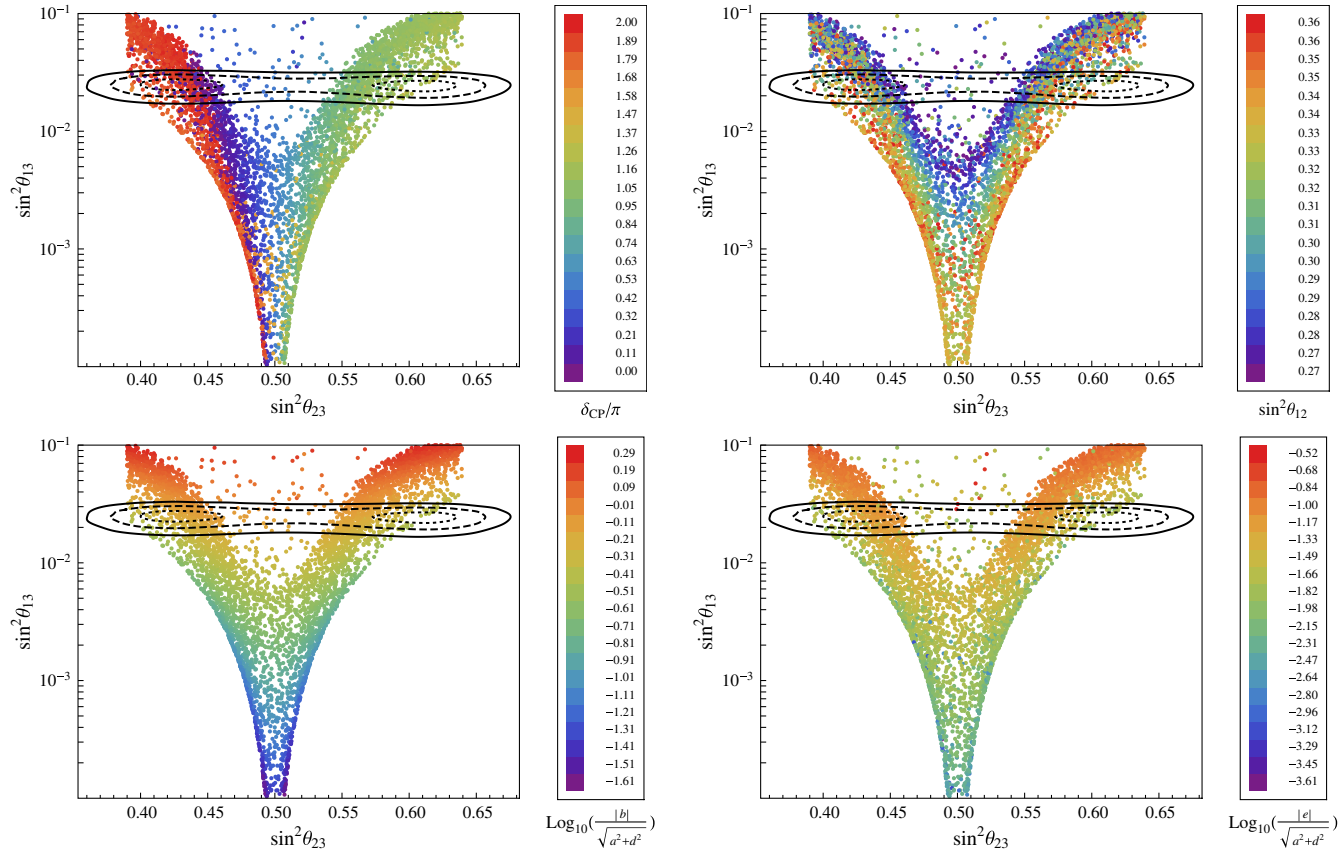

FIG. 3 (color online). Dependence of the reactor angle θ_{13} on the atmospheric mixing angle θ_{23}. The various color codings are given next to each scatter plot. Top left: For $\sin^2\theta_{23} < 1/2 (\sin^2\theta_{23} > 1/2)$ the model predicts $\delta_{CP} = 0$, $2\pi (\delta_{CP} = \pi)$. Top right: The scatterplot shows a band structure in $\sin^2\theta_{12}$. Bottom left: For the points in the experimentally allowed region, $\hat{b}$ has to be of similar size as $\hat{a}$, $\hat{d}$. Bottom right: For the points in the experimentally allowed region, $\hat{e}$ has to be of approximately 1 order of magnitude smaller than $\hat{a}$, $\hat{d}$. The 1, 2, and 3 sigma regions of Ref. [7] are again indicated by dotted, dashed, and continuous contours, respectively.

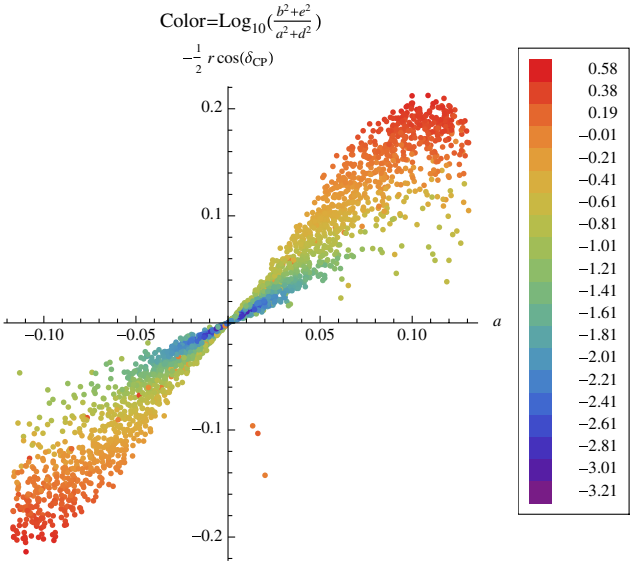

FIG. 4 (color online). Numerical evaluation of the approximate atmospheric sum rule (3.25). The numerical evaluation shows that the sum rule holds to a good degree of approximation.

scan. The color coding gives an indication of the magnitude of deviations from TBM and for small values the approximate relation is fulfilled to good accuracy.

Finally, let us comment on the predictions for neutrinoless double beta decay. As can be read off from Eq. (3.15), the effective Majorana mass of the electron neutrino is given by

$$|m_{ee}| = \left| \hat{a} + \frac{2\hat{d}}{3} + \left(2\hat{e} + \frac{\hat{b}}{3}\right) e^{i\alpha_\lambda} \right|, \tag{3.29}$$

which can be expressed in terms of physical parameters as

$$\begin{aligned} |m_{ee}| &= \left| \sum_i U_{ei}^2 m_i \right| \\ &\approx \frac{2m_1 - m_2}{3} \left| 1 - \frac{2m_1 + 2m_2}{2m_1 - m_2} s \right. \\ &\quad \left. - i \frac{2\delta\varphi_1 m_1 - \delta\varphi_2 m_2}{2m_1 - m_2} \right|. \end{aligned} \tag{3.30}$$

As the additional neutral fermions S do not mix with neutrinos, there is no additional contribution due to the

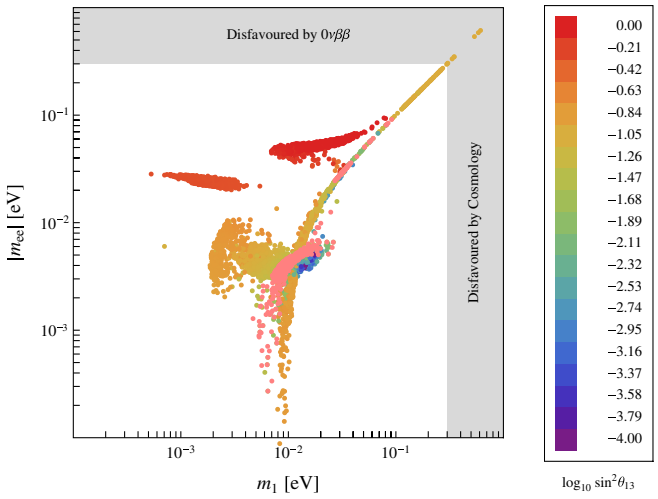

FIG. 5 (color online). Expectation for the effective mass of neutrinoless double beta decay. The pink points lie within the 3 sigma region for all oscillation parameters. The points with color coding lie within the 3 sigma range for all observables except θ_{13}.

heavy singlet, like in Ma's scotogenic model [18,19]. In Fig. 5 we show the predicted range for the effective Majorana mass of the electron neutrino. As can be seen, the scan of parameters prefers moderately large values of the absolute mass scale; however, the effective Majorana mass of the electron neutrino can become small or even vanish.

IV. LEPTON FLAVOR VIOLATION

In models with radiative neutrino mass generation, generally the particles in the loop can also mediate flavor changing processes, in particular, lepton flavor violating rare decays. Before we enter into a detailed discussion of the various processes, we want to remind the reader about the remnant Z_3 symmetry in the charged lepton sector

$$\begin{aligned}(H, \varphi', \varphi'') &\sim (1, \omega^2, \omega),\\ (L_e, L_\mu, L_\tau) &\sim (1, \omega^2, \omega),\\ (e^c, \mu^c, \tau^c) &\sim (1, \omega, \omega^2),\end{aligned} \tag{4.1}$$

which suppresses several LFV rare decays. If the remnant Z_3 would be a symmetry of the whole Lagrangian, only the following LFV rare decays

$$\tau^+ \to \mu^+\mu^+e^- \quad \text{and} \quad \tau^+ \to e^+e^+\mu^-$$

and their charged conjugates would be allowed. All other decays can only proceed through a coupling to the Z_3 breaking VEVs of the neutrino sector. Those decays are naturally suppressed and the symmetry thus protects the model from large constraints. At first, we will discuss the radiative LFV rare decays $l_i \to l_j\gamma$ in Sec. IV A, focusing on the experimentally most well-studied process, namely, the process $\mu \to e\gamma$. In Sec. IV B, we discuss the LFV rare decays with purely leptonic final states, which are allowed at tree level, but suppressed by a three-body final state. Finally, we calculate the anomalous magnetic moment of the muon and compare it to experiment in Sec. IV C.

A. Radiative LFV decays $l_i \to l_j\gamma$

Let us first discuss the process of type $l_i \to l_j\gamma$ using an effective field theory approach. Such processes are described by effective operators of the form [40,41]

$$L\sigma_{\mu\nu}F^{\mu\nu}\ell^c\tilde{H}/M^2 \sim (\underline{\mathbf{3}}_{\mathbf{1}}, 1), \tag{4.2}$$

which transforms in the same way as the mass term under the flavor symmetry. It thus has to be multiplied by flavons to form an invariant. As we already mentioned, the remnant Z_3 symmetry in the charged lepton sector forbids all radiative LFV rare decays. Hence, the effective operator in Eq. (4.2) has to involve VEVs of the neutrino sector in order to lead to nonvanishing decay rates. The lowest order operators that can multiply the mentioned LFV operator in the flavor basis read

$$\Omega_T^\dagger\langle(\phi_1^4)_{\underline{\mathbf{3}}_{\mathbf{1}}}\rangle = \frac{1}{6}(ab(b^2-a^2))(1,1,1)^T, \tag{4.3a}$$

$$\Omega_T^\dagger\langle(\phi_2^4)_{\underline{\mathbf{3}}_{\mathbf{1}}}\rangle = \frac{1}{6}(cd(d^2-c^2))(1,1,1)^T, \tag{4.3b}$$

$$\Omega_T^\dagger\langle(\phi_1^2\phi_2^2)_{\underline{\mathbf{3}}_{\mathbf{1}}}\rangle = \frac{1}{3}(ab(c^2-d^2))(1,1,1)^T, \tag{4.3c}$$

$$\Omega_T^\dagger\langle(\phi_1^2\phi_2^2)_{\underline{\mathbf{3}}_{\mathbf{1}}}\rangle = \frac{1}{3}(cd(a^2-b^2))(1,1,1)^T. \tag{4.3d}$$

There can be more than one contraction, but in the vacuum they all result in these expressions. The lowest order effective operators thus all give contributions that can be written as

$$\begin{aligned}\mathcal{L}_{\text{eff}} &= \mathrm{i}\frac{e}{M^2}\ell^{cT}H^\dagger\sigma_{\mu\nu}F^{\mu\nu}\mathcal{M}L + \text{h.c.} \quad \text{with}\\ \mathcal{M} &= \begin{pmatrix}\alpha_1 & \alpha_1 & \alpha_1\\ \alpha_2 & \alpha_2 & \alpha_2\\ \alpha_3 & \alpha_3 & \alpha_3\end{pmatrix}\frac{\langle\phi_1^4\rangle}{M^4},\end{aligned} \tag{4.4}$$

where α_i are dimensionless couplings that should (naturally) be of order one and the mass scale M is the suppression scale of the higher dimensional operators. Note that the structure of flavor symmetry breaking in the neutrino sector is encoded in $\mathcal{M}$. The symmetry thus automatically leads to a large suppression. From this matrix the LFV transition amplitudes can be determined as [40]

$$\frac{\text{Br}(l_i \to l_j\gamma)}{\text{Br}(l_i \to l_j\nu_i\bar{\nu}_j)} = \frac{12\sqrt{2}\pi^3\alpha}{G_F^3 m_i^2 M^4}(|\mathcal{M}_{ij}|^2 + |\mathcal{M}_{ij}|^2)^2, \tag{4.5}$$

and the magnetic dipole moments a_i and electric dipole moments d_i of the charged leptons are given by [40]

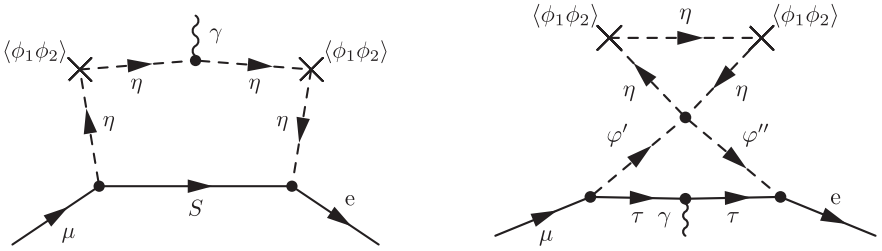

FIG. 6. Lowest order $\mu \to e\gamma$ processes mediated by $\hat{\eta}$ (left) and $\varphi^{\prime(\prime)}$ (right). There has to be a coupling to the VEVs $\langle\phi_1\phi_2\rangle$ of the neutrino sector, which suppresses the amplitudes.

$$a_i = 2m_i \frac{v}{\sqrt{2}M^2} \mathrm{Re}\mathcal{M}_{ii}, \qquad d_i = e\frac{v}{\sqrt{2}M^2} \mathrm{Im}\mathcal{M}_{ii}. \tag{4.6}$$

Note that the matrix $\mathcal{M}$ has additional dominant contributions to the diagonal entries stemming from operators that involve χ instead of $(\phi_i)^4$. Using only the observables $\mu \to e\gamma$, $\tau \to \mu\gamma$ and $\tau \to e\gamma$ as well as charged lepton electric and dipole moments, it is therefore very difficult to test the underlying symmetry pattern, but it can give important indications distinguishing different models. For example, in this model one would expect—barring the possibility of fine-tuned cancellations among the α_i—similar branching ratios for the LFV decays $\mu \to e\gamma$, $\tau \to \mu\gamma$, and $\tau \to e\gamma$, as was also found in SUSY A_4 models [40,42].

In the following, we will focus on $\mu \to e\gamma$, which is the most tightly constrained LFV rare decay. The leading contribution to $\mu \to e\gamma$ is given by the diagram depicted in Fig. 6(a). It is similar to the neutrino mass diagram Fig. 1 in the last section. LFV rare decays mediated by the flavor violating EW doublets $\varphi^{\prime(\prime)}$ are suppressed by one more loop order because of the necessity to couple to the neutrino sector VEVs. Hence, they only show up at two-loop order, as shown in Fig. 6(b). We will therefore not consider this diagram further.

Without any mass insertion along the η line, a one-loop diagram of this type evaluates to [19,43,44]

$$\mathrm{Br}(\mu \to e\gamma) = \frac{3\alpha}{64\pi(G_F m_0^2)^2} C^4, \tag{4.7}$$

where $m_0^2 = \frac{1}{3}(M_1^2 + M_2^2 + M_3^2)$ and, using $x_J = (M^2_{\eta^+})_{JJ}/m_0^2$ and $h_{\alpha kJ} = \frac{\partial \mathcal{L}_\nu}{\partial L_\alpha \partial S_k \partial \hat{\eta}_J}$,

$$C^2 = \left| \sum_{i=1}^{3}\sum_{J=1}^{9} h_{\mu iJ} h^*_{eiJ} x_J^{-2} F_2(M_S^2/(M^2_{\eta^+})_{JJ}) \right| \quad \text{and}$$

$$F_2(t) = \frac{1 - 6t + 3t^2 + 2t^3 - 6t^2 \ln t}{6(1-t)^4}.$$

In our model, we have $C^2 = 0$ for the symmetry reasons given above and there have to be mass insertions to generate flavor violating interactions. Note that this is a welcome feature since LFV processes of this type severely constrain models that generate neutrino masses radiatively [19]. This can be seen as the experimental constraint $\mathrm{Br}(\mu \to e\gamma) < 2.4 \times 10^{-12}$ [45] requires $C^4 \sim 1.5 \times 10^{-8}$ for $M_S = m_0 = 100$ GeV. The flavor symmetry automatically reduces C^2 by a factor $(\frac{\delta M^2_{\eta^+}}{M^2_{\eta^+}})^2$. In the limit $(\frac{\delta M^2_{\eta^+}}{M^2_{\eta^+}})^2 \ll 1$, the diagram in Fig. 6(a) can be computed explicitly, and we find

$$\mathrm{Br}(\mu \to e\gamma) = \frac{\alpha}{16\pi(G_F m_0^2)^2} \tilde{C}^4, \tag{4.8}$$

where

$$\tilde{C}^2 = \frac{1}{m_0^4} \left| \sum_{i=1}^{3}\sum_{J,K,L=1}^{9} h_{\mu iJ} (\delta M^2_{\eta^+})_{JK} (\delta M^2_{\eta^+})_{KL} h^*_{eiL} \times F_4(M_S, M_J, M_K, M_L) \right|, \tag{4.9}$$

and F_4 is a dimensionless loop integral, which we only give in the limit of degenerate η masses

$$\begin{aligned} G_2(t) &\equiv F_4(M_S = tm_0, M_J = m_0, M_K = m_0, M_L = m_0) \\ &= \frac{1}{48(t^2-1)^{12}}[1 - 12t^2 - 36t^4 + 44t^6 + 3t^8 \\ &\quad - 24(2t^2+3)t^4 \ln t]. \end{aligned} \tag{4.10}$$

The dimensionless functions F_2 and G_2 are plotted in Fig. 7. The explicit form of the sum in the expression (4.9)

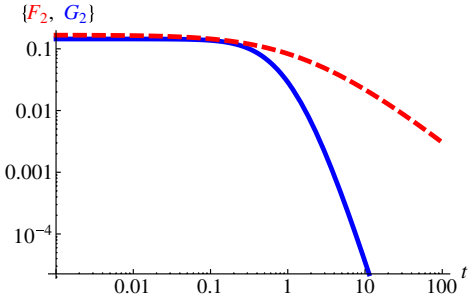

FIG. 7 (color online). The functions F_2 (red dashed) and G_2 (blue solid).

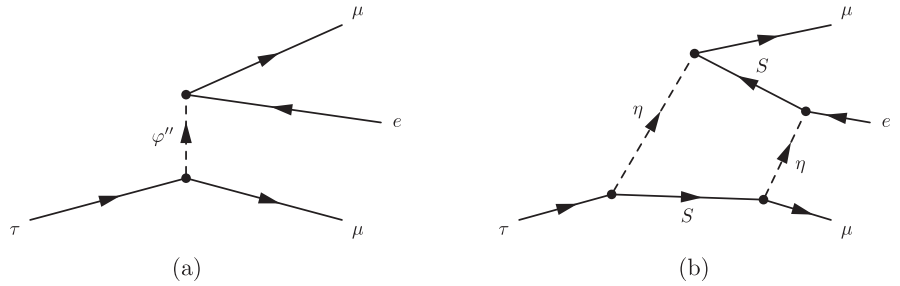

FIG. 8. Lepton flavor violating rare decay $\tau^- \to \mu^-\mu^- e^+$. (a) Tree level contribution of φ''. (b) One-loop contribution of S-η.

for $\tilde{C}^2$ is quite involved and will not be shown here, but it can be easily obtained using Eq. (A10). Here, we only comment on the generic size of the branching ratio. In general, the processes $\mu \to e\gamma$ and the radiative neutrino mass diagram break different approximate symmetries and it is therefore not necessarily the case that the smallness of neutrino masses implies a small branching ratio. This is also the case here. For example, from Eq. (3.14), one can read off that the smallness of neutrino mass could be due to very small values for $\lambda_1 \approx \lambda_2 \approx 10^{-9}$, with all other couplings being order one. Then the dominant contributions to $\tilde{C}^2$ would be of the type

$$\tilde{C}^2 \supset \frac{G_2(t)}{m_0^4}\frac{1}{432}h_2\lambda_4(bc-ad) \times[-h_1\lambda_3(ac+bd)+\omega^2 h_2\lambda_4(bc-ad)], \quad (4.11)$$

where we have again used the limit of degenerate masses $M_i = m_0$, and could in principle be of order one. However, if we stick to the parts of parameter space where the smallness of neutrino mass is due to many moderately small couplings h_i, $\lambda_i \sim \mathcal{O}(0.01\text{–}0.1)$ and $m_0 \sim \mathcal{O}(\text{TeV})$, $\langle\chi\rangle$, $\langle\phi_i\rangle \sim \mathcal{O}(100\ \text{GeV})$ [as discussed below (3.14)] instead of one very small coupling, the branching ratio is heavily suppressed by $\tilde{C}^4 \sim (10^{-9}\text{–}10^{-13})^2$. These natural parameter values thus give an appealing explanation of both the smallness of neutrino masses and the suppression of LFV decays.

B. LFV decays $l_i \to lll$

Another class of processes that are of interest for our model are rare flavor violating decays of the type $\mu \to eee$. As in the case of the processes $f_i \to f_j\gamma$ the allowed decay channels are restricted by the flavor symmetry. If we do not consider the heavily suppressed diagrams that couple to VEVs in the neutrino sector, it is clear that the process $\mu \to eee$ is not allowed by the Z_3 symmetry of the charged lepton sector and the most constraining process is given by $\tau^- \to \mu^-\mu^- e^+$.

This process can be mediated at tree level by the neutral components of φ'' as depicted in Fig. 8(a) and its branching ratio is given by [22,24]

$$\mathrm{Br}(\tau^- \to \mu^-\mu^- e^+) = \left(\frac{36 m_\tau^2 m_\mu^2}{M_0^4}\right) \times \mathrm{Br}(\tau \to \mu\nu\nu) = 1.7\times 10^{-8}\left(\frac{62\ \text{GeV}}{M_0}\right)^4, \quad (4.12)$$

where we have used $\mathrm{Br}(\tau \to \mu\nu\nu) = 0.174$. Compared to the experimental upper bound of 1.7×10^{-8} [34], the effective mass[7]

$$\frac{1}{M_0^4} = \left[\frac{\sin^2\alpha}{m_{\Phi_1}^2} + \frac{\cos^2\alpha}{m_{\Phi_2}^2}\right]^2 \quad (4.13)$$

is thus only weakly constrained. All other processes mediated by $\varphi'^{(\prime)}$ are further suppressed by $y_e y_\tau$ or $y_\mu y_e$. Rare LFV processes mediated by these fields are therefore naturally suppressed by smallish Yukawa couplings and do not put a serious constraint on the model.

Let us also estimate the magnitude of the diagram in Fig. 8(b) mediating $\tau \to \mu\mu e$, as this diagram may in principle be larger because it is not suppressed by Yukawa couplings that are known to be small.

To get an estimate, we work in the limit of degenerate η masses $M_1 = M_2 = M_3 = m_0$ and find

$$\Gamma(\tau^- \to \mu^-\mu^- e^+) \sim \left|\frac{1}{16\pi^2}\sum_{j,k=1}^{9}\sum_{i,l=1}^{3} h_{\tau ij}h^*_{\mu ik}h_{elk}h^*_{\mu lj}\frac{H(M_S/m_0)}{m_0^2}\right|^2,$$

where $H(M_S/m_0)$ is a dimensionless loop integral and

$$\mathrm{Br}(\tau^- \to \mu^-\mu^- e^+) = \mathrm{Br}(\tau \to \mu\nu\nu)\frac{\Gamma(\tau^- \to \mu^-\mu^- e^+)}{\Gamma(\tau^- \to \mu^-\bar{\nu}_\mu\nu_\tau)}.$$

Evaluating the sum, we find $\sum_{j,k=1}^{9}\sum_{i,l=1}^{3} h_{\tau ij}h^*_{\mu ik} \times h_{elk}h^*_{\mu lj} = \frac{1}{27}(h_1^4 - h_1^2h_2^2 + h_2^4)$, and the experimental bound

[7] In Ref. [22] $\lambda_{\chi A} = 0$ was assumed, which implies $\alpha = \pi/4$.

$$\mathrm{Br}(\tau^- \to \mu^-\mu^-e^+) = \left|\left(\frac{159\ \mathrm{GeV}}{m_0}\right)^2 (h_1^4 + h_2^4 - h_1^2h_2^2) H(M_S/m_0)\right|^2 \cdot 1.7 \times 10^{-8} \tag{4.14}$$

can easily be evaded even for small values of $m_0 \sim 178\ \mathrm{GeV} \approx 308/\sqrt{3}\ \mathrm{GeV}$ (which would give the correct dark matter relic abundance of η in the degenerate limit we are considering here, as will be discussed in Sec. V B) and order one Yukawas [assuming $H(M_S/m_0) \sim 1$]. For the parameter ranges preferred by one-loop neutrino mass generation, i.e., $h_i \sim 0.1$, the expected branching ratio is too small to expect a signal in next-generation experiments. In summary, we can conclude that the flavor symmetry effectively protects against lepton flavor violating interactions.

C. Anomalous magnetic moment of muon

Let us now briefly discuss the anomalous magnetic moment of the muon. The contribution from the exchange of the neutral component of φ'' should give the largest contributions, as it is proportional to the tau Yukawa coupling squared. It has been calculated previously [17] and amounts to

$$\Delta a_\mu = \frac{G_F m_\tau^2}{2\sqrt{2}\pi^2}\left(\frac{m_\mu^2}{M_0^2}\right) = 1.5 \times 10^{-12}\left(\frac{100\ \mathrm{GeV}}{M_0}\right)^2, \tag{4.15}$$

which is negligible and cannot account for the reported deviation of $(290 \pm 90) \times 10^{-11}$ [46,47], from the Standard Model. The charged components of η also contribute to the anomalous magnetic moment of the muon, with a strength given by [43,47]

$$\begin{aligned}\Delta a_\mu &= -\frac{m_\mu^2}{3(4\pi^2)^2}\left[\frac{h_1^2}{M_1^2}F_2\left(\frac{M_S}{M_1}\right) + \frac{h_2^2}{M_2^2}F_2\left(\frac{M_S}{M_2}\right)\right] \\ &= -1.8 \times 10^{-12}\sum_i \left(\frac{h_i}{0.1}\right)^2\left(\frac{100\ \mathrm{GeV}}{M_i}\right)^2\left(\frac{F_2(\frac{M_S}{M_i})}{F_2(1)}\right).\end{aligned} \tag{4.16}$$

This therefore gives a very mild constraint on the masses and Yukawa couplings of the η's. In the preferred parameter space for neutrino mass generation, this contribution is negligible. Note that the contribution goes in the opposite direction of the reported excess and it can therefore not be used to explain it [43].

V. DARK MATTER

In this section we discuss dark matter candidates of the model and their phenomenology.

A. Dark matter candidates and their stability

To start off the discussion of possible dark matter candidates in our model, let us dwell on the remnant symmetries left over after symmetry breakdown. While the $Q_8 \rtimes A_4$ part of the symmetry group is completely broken,[8] there is a Z_2 symmetry given by

$$\mathcal{R}: L \to -L \qquad \ell^c \to -\ell^c \qquad \eta_i \to -\eta_i, \tag{5.1}$$

which is the $(-1)^{L'}$ remnant of the auxiliary Z_4 symmetry $i^{L'}$, where $L' = L + N_\eta$ is the generalized lepton number symmetry that is the sum of the usual SM lepton number with the η number N_η. At the renormalizable level after symmetry breaking, there is another Z_2 symmetry of the model given by

$$\mathcal{A}: S \to -S \qquad \eta_i \to -\eta_i. \tag{5.2}$$

This is purely an accidental symmetry that emerges due to the particle content and the requirement of renormalizability and not a remnant of some symmetry we have imposed on the model. The reason why it emerges can be traced back to the fact that the SM fermions as well as χ transform only under the generators S and T that form the subgroup A_4, and thus there are no operators of the form $\varphi\mathcal{O}_{A_4}$, where φ is a field transforming nontrivially under X (e.g., fields transforming as $\underline{\mathbf{3_i}}$ with $i \neq 1$ such as S and η) and $\mathcal{O}_{A_4}$ is an arbitrary operator formed by fields transforming under A_4. The symmetry $\mathcal{A}$ makes the lightest component of S and η stable, which implies that the dark matter candidate is either fermionic or bosonic. This symmetry, however, is only an accidental symmetry and there is thus no reason for higher dimensional operators to respect this symmetry. Such a higher dimensional operator $\mathcal{O}$ with $\mathcal{A}[\mathcal{O}] \neq \mathcal{O}$ would lead to a decay of the dark matter candidate. On the contrary, all higher dimensional operators have to respect the symmetry $\mathcal{R}[\mathcal{O}] = \mathcal{O}$, as this symmetry is a remnant of an exact symmetry and is therefore also exact. We will now show that this requirement pushes up the dimensionality of the higher dimensional decay operators to a level where the dark matter candidate is stable for all practical purposes. Since the discussion depends on whether the dark matter candidate stems from η or from S, we discuss the two possibilities in turn.

1. Scalar DM

Any effective operator that would mediate a decay of the lightest component of η_i has to be of the form

$$\mathcal{O} = \eta_i \mathcal{O}_{\mathrm{SM}}^{\Delta L=1}\langle\mathcal{O}_{\phi_k\phi_l}\rangle, \tag{5.3}$$

[8]There have been several studies of dark matter, which is stabilized by a remnant subgroup of a flavor symmetry [48], while it is completely broken in our model.

where $\langle \mathcal{O}_{\phi_k\phi_l} \rangle$ is built out of SM-singlet flavon fields and transforms even under $\mathcal{R}$. As η is odd under $\mathcal{R}$, the operator $\mathcal{O}_{\mathrm{SM}}^{\Delta L=1}$, which is built up of SM fields, has to be also odd under $\mathcal{R}$ to make the complete operator invariant. Obviously the complete operator $\mathcal{O}$ is odd under the accidental symmetry $\mathcal{A}$ and thus mediates DM decay.

Since $\mathcal{R}$ acts upon SM particles as the discrete subgroup of lepton number $(-1)^L$, the operator $\mathcal{O}_{\mathrm{SM}}^{\Delta L=1}$ has to violate lepton number by an odd unit and has to transform as an electroweak doublet. The lowest dimensional operators in the SM arise at dimension six and violate L by one unit (see Ref. [49] for a recent review of gauge invariant dimension six operators)

$$L u^c d^c d^c \qquad \bar{L}\bar{d}^c\bar{d}^c\bar{d}^c \qquad L\bar{Q}\,\bar{Q}\,d^c \qquad \bar{e}^c\bar{Q}d^c d^c \tag{5.4a}$$

$$\chi^\dagger L Q Q Q \qquad \chi^\dagger e^c u^c u^c d^c \qquad \chi^\dagger \bar{L}\,\bar{Q}\,u^c d^c \qquad \chi^\dagger \bar{e}^c Q Q \bar{u}^c \qquad \chi^\dagger L Q \bar{u}^c \bar{d}^c. \tag{5.4b}$$

All dimension six operators in Eq. (5.4a) break baryon number by one unit, $B-L$ by two units, and preserve $B+L$. The dimension seven operators in Eq. (5.4b) on the other hand break baryon number by one unit, preserve $B-L$, and break $B+L$ by two units. They are formed by adjoining χ to a dimension six proton decay operator. Since baryon number is an accidental symmetry in our model (in the same way as in the Standard Model), these operators are never generated[9] within the model and thus dark matter is stable within the model. They rather parametrize some baryon number violating physics, which from proton decay experiments is pushed to scales of the order of $\Lambda_B \approx 10^{16}$ GeV.

To form a singlet under the flavor symmetry, the second operator $\mathcal{O}_{\phi_k\phi_l}$ is needed to make the total operator $\mathcal{O}$ a singlet under the flavor symmetry, as η_i transforms under X while $\mathcal{O}_{\mathrm{SM}}^{\Delta L=1}$ does not. It has to be composed of an even number of flavons ϕ_k, as under the Z_2 subgroup generated by[10] X^2 only ϕ_k transforms nontrivially.

If we assume the presence of baryon number violating operators at scale Λ_B, the dark matter candidate η decays into quarks and one lepton. Under the assumption that the flavor part of the operator is related to the breaking of the flavor symmetry Λ_F, a DM decay operator formed by a dimension six SM operator $\mathcal{O}_{\mathrm{SM}}^{\Delta L=1}$ is suppressed by Λ_B^3:

$$\frac{\eta_i \mathcal{O}_{\mathrm{SM}}^{\Delta L=1}}{\Lambda_B^3}\frac{\langle\phi_k\phi_l\rangle}{\Lambda_F^2}. \tag{5.5}$$

Hence, the lifetime of DM can be estimated to be

$$\Gamma^{-1} \sim \frac{8\pi\Lambda_B^6}{m_\eta^7}\left(\frac{\Lambda_F^2}{\langle\phi_k\phi_l\rangle}\right)^2 = 1.9\times10^{45}\,\mathrm{Gyr}\left(\frac{\Lambda_B}{10^{16}\,\mathrm{GeV}}\right)^6 \times\left(\frac{100\,\mathrm{GeV}}{m_\eta}\right)^7\left(\frac{\Lambda_F^2}{\langle\phi_k\phi_l\rangle}\right)^2 \tag{5.6}$$

and the dark matter candidate is thus stable even on cosmological time scales, if one assumes "traditional" values for the scale of baryon number violating physics. However the operators in Eq. (5.4a) are not those directly tested in proton decay experiments and the physics of baryon number violation might be such that the operators in Eq. (5.4a) are suppressed by a smaller energy scale than the one responsible for baryon decay. We will come back to the issue of induced proton decay at the end of the subsection, but now we want to turn the logic around and derive bounds on Λ_B and Λ_F from the fact that dark matter is still around.

Decaying DM models are constrained by WMAP to $\Gamma^{-1} \geq 123$ Gyr at 68% C.L. [50] and WMAP + SN Ia to $\Gamma^{-1} \geq 700$ Gyr at 95.5% C.L. [51]. Furthermore, decaying DM is constrained by possible neutrino final states [52], which serve as a conservative limit, since neutrinos are the least detectable SM particles. The exact bound depends on the DM mass ranging from 10^{22} s $= 10^8$ Gyr at $\mathcal{O}(1$ GeV) and increasing almost linearly on a log-log plot to 10^{28} s $\approx 10^{14}$ Gyr at $\mathcal{O}(100$ TeV). Diffuse gamma ray constraints from Fermi data yield a limit of $\Gamma^{-1} \gtrsim 10^{26}$ s $\approx 10^{12}$ Gyr [53] for the decay into a pair of charged leptons. Here, DM decays into one lepton and quarks, which might lead to further softer leptons in the final state. Hence the bounds do not directly apply, but we will use it to obtain an order of magnitude estimate for the suppression scale of the lowest order DM decay operator in Eq. (5.3). Using the limit from diffuse gamma rays with $\Gamma^{-1} \gtrsim 10^{26}$ s as a benchmark value, we obtain a limit on the suppression scale of

$$(\Lambda_B^3\Lambda_F^2)^{1/5} \gtrsim 6\times10^7\ \mathrm{GeV}\left(\frac{m_\eta}{1\ \mathrm{TeV}}\right)^{7/10}\left(\frac{\langle\phi_k\phi_l\rangle}{(100\ \mathrm{GeV})^2}\right)^{1/5}. \tag{5.7}$$

Because of the high dimensionality of the operator, the bound on the suppression scale $\Lambda_{B,F}$ does not depend strongly on the bound on the lifetime.

All of the operators in Eq. (5.4) lead to DM induced proton decay[11] into a final state lepton and final state mesons

[9] Except through instantons and sphalerons, which do not play a role here, in the same way as in the SM.

[10] This element generates the center of the group and thus commutes with all group elements.

[11] Induced proton decay has been studied in the context of asymmetric DM [54]. However, their analysis does not apply in our case, because the induced proton decay is mediated via a different operator with different kinematics, since one of the final state particles has a nonnegligible mass of the order of the proton mass.

$$\eta_i + N \longrightarrow L + M. \tag{5.8}$$

As the proton as well as the DM are nonrelativistic and they annihilate at rest, the induced proton decay leads to similar kinematics as in the ordinary proton decay, but the total rest energy $E \sim m_\eta + m_N \approx m_\eta$ is much larger compared to the ordinary proton decay with $E \sim m_N$. Hence, the final state particles appear to originate from the decay of a much heavier particle and the experimental signatures change. Therefore, the existing limits on proton decay are not directly applicable. However, in generic grand unified theory models, for example, the operators given in Eqs. (5.4a) and (5.4b) and the proton decay operators are generated at the same energy scale.

2. Fermionic DM

Similarly to scalar DM consisting of the lightest component of η_i, S can decay via higher dimensional operators. They are generally of the form

$$S\mathcal{O}_{\rm SM}\langle\mathcal{O}_{\phi_k\phi_l}\rangle, \tag{5.9}$$

where $\mathcal{O}_{\rm SM}$ transforms like a spin $\frac{1}{2}$ fermion, which is a singlet under the SM group, but transforms nontrivially under the flavor symmetry.[12] The lowest dimensional operators $\mathcal{O}_{\rm SM}$ emerge at dimension $\frac{9}{2}$

$$u^c d^c d^c \qquad \bar{Q}\,\bar{Q}\,d^c \qquad \chi Q \bar{u}^c \bar{d}^c \qquad \chi QQQ. \tag{5.10}$$

Note that these operators transform trivially under $\mathcal{R}$, as does S. All of these operators violate baryon number by one unit, and therefore they lead to induced proton decay. However, the kinematics is quite different compared to ordinary proton decay, because the lowest order operators do not contain a final state lepton.

Similarly to the scalar case, there are bounds from astrophysical observations. As DM decay only arises at dimension eight, the bound on the suppression scale does not depend strongly on the exact bound on the lifetime. Therefore, we again make a rough estimate of the bound on the suppression scale by using the same lifetime as in the scalar case, and we obtain

$$(\Lambda_B^2\Lambda_F^2)^{1/4} \gtrsim 9\times 10^8\ \text{GeV}\left(\frac{m_\eta}{1\ \text{TeV}}\right)^{5/8}\left(\frac{\langle\phi_k\phi_l\rangle}{(100\ \text{GeV})^2}\right)^{1/4}, \tag{5.11}$$

due to the lower dimensionality of the DM decay operator.

B. Dark matter phenomenology

We now give a brief overview of the phenomenology of the two different dark matter candidates. We will estimate the DM abundance and detection possibilities for the different scenarios and show that there is a region of parameter space where the correct abundance can be obtained. A detailed calculation is beyond the scope of the present work. Again, we discuss the different dark matter candidates separately.

1. Scalar DM

The scalar dark matter candidate is a component of an inert EW doublet. Therefore, we are going to translate the analysis for scalar multiplet DM done in Ref. [55] to our setup. A detailed analysis would require the precise calculation of the η_i mass matrices. We assume that one of the triplets η_i is sufficiently lighter than the other two, such that we do not have to take them into account during freeze-out of DM, i.e., they have to be at least 20% heavier than the DM candidate [56]. In the following, we will denote the triplet containing the DM candidate by $\eta_{\rm DM}$ with direct mass term $M_{\eta_{\rm DM}}$. We are going to assume, as we did previously in the section about the neutrino masses, that the direct mass term $M_{\eta_{\rm DM}}$ dominates over all mass terms induced by VEVs. Hence, the DM mass is approximately given by the direct mass term $M_{\eta_{\rm DM}}$. In the limit that the mass splittings are below 1%, we can neglect the annihilations via other scalars and concentrate on the pure gauge (co)annihilation channels. Following Ref. [55], there is an upper bound on the DM mass of an inert doublet of $m^* = 534 \pm 25\ \text{GeV}(3\sigma)$ from overclosing the Universe in this limit. The correct DM abundance is obtained for m^*. As $\eta_{\rm DM}$ is in a triplet representation of $Q_8 \rtimes A_4$, there are three almost degenerate doublets, which all contribute to the DM density equally. Therefore, the upper bound on the DM mass is lowered by approximately a factor of $\sqrt{3}$ to $m_\eta^* \approx 308$ GeV, which is consistent with direct searches for scalar particles, as discussed in Sec. VII.

Today, the mass splitting between DM and the next-to-lightest particles forbids gauge interactions kinematically due to the small DM velocities, unless it is tuned to be very small [$\lesssim \mathcal{O}(100)$ keV], and DM can only be detected via the couplings to scalars, specifically via the Higgs portal. The spin-independent cross section for scattering of DM off the neutron is given by [57]

$$\begin{aligned}\sigma_n &\approx \frac{|\lambda_L|^2}{\pi}\frac{\mu^2}{M_{\rm DM}^2}\frac{m_p^2}{m_H^4}f^2 \\ &\approx 2.7\times 10^{-48}\left(\frac{\lambda_L}{0.01}\right)^2\left(\frac{300\ \text{GeV}}{M_{\eta_{\rm DM}}}\right)^2 \\ &\quad\times\left(\frac{125\ \text{GeV}}{m_H}\right)^4\left(\frac{f}{0.3}\right)^2\ \text{cm}^2,\end{aligned} \tag{5.12}$$

with λ_L being the coupling of DM to the Higgs, μ the reduced mass of the DM-neutron system, m_p the mass of the nucleon, m_H the mass of the Higgs, and f parametrizes the nuclear matrix element, $0.14 < f < 0.66$, which we took from Ref. [57]. The estimated cross section is well

[12]Note that S transforms under the symmetry generator X, while $\mathcal{O}_{\rm SM}$ does not. Therefore the operator $\langle\mathcal{O}_{\phi_k\phi_l}\rangle$ is needed to form a singlet.

below the current experimental limits by XENON100 [58], which is the most sensitive DM direct detection experiment in this mass region.

Note, the discussed parameter point is only an example that proves the possibility of obtaining the correct DM relic density. For larger mass splittings, the annihilation via scalar interactions cannot be neglected in the calculation of the DM relic abundance, and the direct detection cross section is enhanced.

2. Fermionic DM

For the discussion of the fermionic DM candidate contained in S, we follow the discussion in Ref. [19] to show that it is possible to obtain the correct relic abundance. For completeness, we repeat the relevant steps with the necessary changes. At tree level, there is only the mass term $\sqrt{3}M_S SS = M_S(S_1^2 + S_2^2 + S_3^2)$ and thus all components of S are degenerate. At loop level this degeneracy is lifted and for concreteness we here take $M_{\tilde{S}_3} \gtrsim M_{\tilde{S}_2} \gtrsim M_{\tilde{S}_1}$, where $\tilde{S}_i$ are mass eigenstates. The states $\tilde{S}_{2,3}$ can decay into $\tilde{S}_1$ and leptons by the interchange of η and thus at the present time only $\tilde{S}_1$ is around. However, due to the near degeneracy, the freeze-out of all three species runs in parallel. Coannihilation processes of the type $S_i S_j \to \mathrm{SM}$ with $i \neq j$ are suppressed in comparison to annihiliation processes $S_i S_i \to \mathrm{SM}$, because they require an additional mass insertion along the η line. It is thus a very good approximation to consider the freeze-out of each component separately and the total relic abundance is thus just given by the sum of the abundances of S_1, S_2, and S_3.

The annihilation cross section for each S_k into leptons in the limit of vanishing lepton masses and scalar mass splittings [59] is given by

$$\begin{aligned}\langle \sigma v \rangle &= b v^2 + \mathcal{O}(v^4),\\ b &= \sum_{i=1,2} \frac{h_i^4 r_i^2 (1 - 2r_i + 2r_i^2)}{24\pi M_S^2},\\ r_i &= \frac{M_S^2}{M_i^2 + M_S^2}.\end{aligned} \tag{5.13}$$

In the limit of $M_S \ll M_i$, the expression for the p wave simplifies to

$$b = \frac{M_S^2}{24\pi} \sum_{i=1,2} \left(\frac{h_i}{m_i}\right)^4, \tag{5.14}$$

i.e., the cross section scales with $(h_i/m_i)^4$. The relic density of the SM singlets S, taking into account the mass degeneracy of the components of S, can then be obtained from [60]

$$\Omega_S h^2 = \frac{n_S^0 M_S}{\rho_c} h^2, \tag{5.15}$$

with n_S^0 being the number density of S today, which is

$$(n_S^0)^{-1} = \left(\sum_k n_{S_k}^0\right)^{-1} = \left(3 n_{S_k}^0\right)^{-1} = \frac{0.088 g_*^{1/2} M_{Pl} M_S 3b}{x_f^2 s_0}, \tag{5.16}$$

where $s_0 = 2970/\mathrm{cm}^3$ is today's entropy density, the critical density is $\rho_c = 3H^2/(8\pi G) = 1.05 \times 10^{-5}\ h^2 \mathrm{GeV/cm}^3$, the Planck mass $M_{\mathrm{Pl}} = 1.22 \times 10^{19}$ GeV, and the dimensionless Hubble parameter h. At the freeze-out temperature, the ratio $x_f = M_S/T$ is determined by

$$x_f = \ln \frac{0.0764 M_{\mathrm{Pl}} (6b/x_f) c(2 + c) M_S}{(g_* x_f)^{1/2}} \tag{5.17}$$

with the effective number of degrees of freedom g_* at freeze-out. After eliminating the cross section with Eqs. (5.16) and (5.15), we obtain

$$x_f = \ln \frac{1.74 x_f^{1/2} s_0 h^2 c(2 + c) M_S}{g_* (\Omega_S h^2) \rho_c}. \tag{5.18}$$

Following the discussion in Refs. [19,60], we rewrite Eqs. (5.15) and (5.18) as

$$\left[\frac{M_S}{\mathrm{GeV}}\right] = 1.95 \times 10^{-8} x_f^{-1/2} e^{x_f} \left[\frac{\Omega_d h^2}{0.12}\right], \tag{5.19a}$$

$$\left[\frac{b}{\mathrm{GeV}^{-2}}\right] = 7.32 \times 10^{-11} x_f^2 \left[\frac{\Omega_d h^2}{0.12}\right], \tag{5.19b}$$

using $g_*^{1/2} = 10$ and $c = 1/2$. We solve these equations numerically for fixed values of $h_1 = h_2$ and $M_1 = M_2$ and show the resulting contour lines with the correct DM relic abundance in the plane $M_1/h_1 = M_2/h_2$ vs M_S in Fig. 9. Hence, it is possible to obtain the correct DM relic abundance for fermionic DM, although large Yukawa couplings h_i are required. Similarly to the scalar DM scenario, we expect the cross section to raise with nonvanishing mass

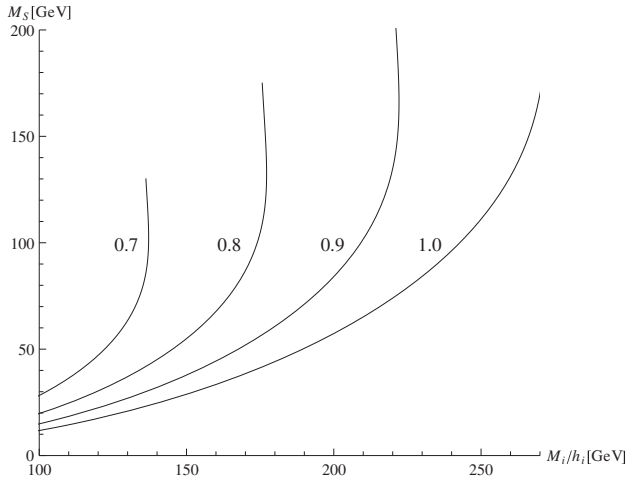

FIG. 9. Contour lines for different values of $h_1 = h_2$ with the correct DM abundance $\Omega_S h^2 = 0.12$.

splittings of the scalars η_i, which allows for smaller Yukawa couplings h_i.

VI. EXTENSION TO QUARK SECTOR

So far we restricted ourselves to the discussion of the flavor structure in the lepton sector. Given the different structures in the lepton and quark sector, one might wonder whether and how this model can be extended to the quark sector. In the following, we will discuss a few simple possibilities to incorporate the quark sector without enlarging the flavor group. It is necessary to specify how quarks transform under the flavor symmetry as this will to a certain extent determine the collider signatures of the model. Alternatively, it is interesting to look for a group extension of the flavor group, which preserves the structure in the lepton sector, but allows for new structure in the quark sector [32]. Here, a viable extension of the full flavor group $Q_8 \rtimes A_4$ is the group $Q_8 \rtimes T' \cong \mathrm{SG}(192, 1022)$ [32] being the analogue of the extension of A_4 to T', which has been used to explain the flavor structure of quarks and leptons simultaneously [61]. A detailed discussion of quark flavor observables is postponed to future work.

A. Quark sector mirroring the lepton sector

We can use the same assignment for the quarks as for the leptons with respect to $(Q_8 \rtimes A_4) \times Z_4$, i.e.,

$$\begin{aligned} Q \sim (\underline{\mathbf{3}}_{\mathbf{1}}, 1), \qquad u^c + c^c + t^c \sim (\underline{\mathbf{1}}_{\mathbf{1}} + \underline{\mathbf{1}}_{\mathbf{2}} + \underline{\mathbf{1}}_{\mathbf{3}}, 1), \\ d^c + s^c + b^c \sim (\underline{\mathbf{1}}_{\mathbf{1}} + \underline{\mathbf{1}}_{\mathbf{2}} + \underline{\mathbf{1}}_{\mathbf{3}}, 1). \end{aligned} \tag{6.1}$$

This assignment leads to the following Yukawa couplings in the Lagrangian:

$$\begin{aligned} -\mathcal{L}_q = {} & y_u Q \chi u^c + y_c Q \chi c^c + y_t Q \chi t^c + y_d Q \tilde{\chi} d^c \\ & + y_s Q \tilde{\chi} s^c + y_b Q \tilde{\chi} b^c + \mathrm{H.c.}, \end{aligned} \tag{6.2}$$

which amount to the mass matrices of the quarks

$$\begin{aligned} M_U &= \frac{v}{\sqrt{2}} \Omega_T^* \mathrm{diag}(y_u, y_c, y_t) \quad \text{and} \\ M_D &= \frac{v}{\sqrt{2}} \Omega_T^* \mathrm{diag}(y_d, y_s, y_b). \end{aligned} \tag{6.3}$$

Hence there is no mixing in the quark sector, i.e., the Cabibbo-Kobayashi-Maskawa (CKM) mixing matrix $V_{\mathrm{CKM}} \equiv V_d^\dagger V_u = \mathbb{1}$, which is a good leading order approximation. The Cabibbo angle can be produced by a cross-talk of operators from the neutrino sector [29], e.g., the operator $(Q\tilde{\chi}d^c)_{\underline{\mathbf{1}}_{\mathbf{2}}}(\phi_1\phi_2)^2/M^4$ leads to a nonvanishing Cabibbo mixing angle. It has to be of the order $(\phi_1\phi_2)^2/(M^4) \sim 10^{-4}(m_s/95\ \mathrm{MeV})$, in order to generate a large enough mixing in the down-type quark sector to explain the Cabibbo angle. Within the model, the operator can be generated at one loop with $\varphi'^{(\prime)}$ running in the loop. However, the contribution turns out to be too small and a different mechanism is required to generate this operator.

Flavor changing neutral currents are naturally suppressed at the leading order, since there is a selection rule $\Delta D \Delta S \Delta B = \pm 2$ as well as $\Delta U \Delta C \Delta T = \pm 2$ in the flavor basis for four Fermi operators similarly to the lepton sector. It has been claimed in Ref. [22] that leptonic Kaon decays result in a relatively strong bound of $M_0 > 510$ GeV on the effective mass M_0 defined in Eq. (4.13). However, there is an error in the calculation. The final result should not depend on the Kaon mass m_K but m_μ and the corrected expression in our model reads

$$\frac{\Gamma(K_L^0 \to \mu^\pm e^\mp)}{\Gamma(K^+ \to \mu^+ \nu)} = \frac{9 m_\mu^2 m_s^2}{|V_{us}|^2} \left[\frac{\sin^2\alpha}{m_{\Phi_1}^2} + \frac{\cos^2\alpha}{m_{\Phi_2}^2} \right]^2. \tag{6.4}$$

The branching fraction is constrained to be less than 4.7×10^{-12}. Using $m_s = 95$ MeV, $m_\mu = 106$ MeV, $V_{us} = 0.225$, this leads to a bound of

$$\frac{m_{\Phi_1} m_{\Phi_2}}{\sqrt{m_{\Phi_1}^2 \cos^2\alpha + m_{\Phi_2}^2 \sin^2\alpha}} \gtrsim 248\ \mathrm{GeV}. \tag{6.5}$$

B. Quarks transforming under generator X

Another interesting possibility that is not possible in A_4 models is to assign the quarks to representations that also transform under the group generator X. Since the top mass is large, we want it to be generated at the renormalizable level, while all the other quark masses might well be the result of higher order effects. Looking at the multiplication rule

$$\underline{\mathbf{3}}_{\mathbf{i}} \times \underline{\mathbf{3}}_{\mathbf{j}} = \sum_{\substack{k=1 \\ k \neq i,j}}^{5} \underline{\mathbf{3}}_{\mathbf{k}} \qquad (i \neq j), \tag{6.6}$$

it is clear that if one assigns $Q \sim (\underline{\mathbf{3}}_{\mathbf{2}}, 1)$ and $U^c \sim (\underline{\mathbf{3}}_{\mathbf{3}}, 1)$ there is only one Yukawa coupling at the renormalizable level

$$-\mathcal{L}_t = y_t Q \chi U^c + \mathrm{H.c.}, \tag{6.7}$$

which generates the top mass. The charm and up quark masses, as well as up sector mixing are generated by operators of the form

$$\begin{aligned} -\mathcal{L}_u = {} & y_i^{(u,1)} [Q \chi U^c (\phi_1 \phi_1)]_i \\ & + y_i^{(u,2)} [Q \chi U^c (\phi_2 \phi_2)]_i + \mathrm{H.c.}, \end{aligned} \tag{6.8}$$

where the sum goes over all singlet contractions of the fields. There are certainly enough parameters to fit the quark masses and up-type mixing. Actually, there are no further predictions besides the large top mass, since there are too many free parameters.

In the down-type sector we can either utilize the same structure as in the up-type sector or, as the bottom quark mass is closer to the charm mass than to the top mass, we

can use the assignment $D^c \sim (\underline{\mathbf{3}}_{\mathbf{1}}, 1)$. With this choice there is no tree-level operator of type (6.7) allowed and all down type quark masses and mixing arise from

$$-\mathcal{L}_u = y_i^{(d,1)}[Q\chi D^c(\phi_1\phi_1)]_i + y_i^{(d,2)}[Q\chi D^c(\phi_2\phi_2)]_i + \text{H.c.} \quad (6.9)$$

We will not discuss this possibility further here, as we are primarily focused on the lepton sector.

C. Additional EW Higgs doublet $H_q \sim \underline{\mathbf{1}}_{\mathbf{1}}$

Another possibility is that the flavor structure in the quark sector could be completely unrelated to the one in the lepton sector. In particular, the quarks might not transform under the flavor symmetry in the lepton sector. This can be simply achieved by assigning the quarks to the singlet representation of the flavor group. In order to generate the quark mass matrices, we have to introduce an additional EW Higgs Doublet H_q, which does not transform under the flavor group. Hence, the flavor structure in the quark sector is unchanged compared to the SM one. Therefore, we do not discuss this possibility further and we will only briefly comment on its collider phenomenology in Sec. VII.

The only effect[13] of the additional Higgs doublet on the discussion in the preceding sections is to rescale the VEV of H such that

$$\langle H^0\rangle^2 + \langle H_q^0\rangle^2 = \frac{1}{2}(\sqrt{2}G_F)^{-1} = \frac{1}{2}(246\ \text{GeV})^2$$

is maintained.

VII. COLLIDER PHENOMENOLOGY

Our model predicts several new particles with EW charges at the EW scale. In this section, we will concentrate on the simplest extension to the quark sector given in Sec. VI A, where quark doublets are assigned to the triplet representation $\underline{\mathbf{3}}_{\mathbf{1}}$ of the flavor group and obtain their masses from a coupling to the flavored Higgs χ, as discussed in the previous section. We will briefly comment on the possibility to have a separate Higgs for the quark sector in Sec. VII E. Besides the fermionic singlets S, there are several EW doublets, which can be grouped in three different categories, the Higgs h, which obtains a VEV, the two partners of the Higgs in the flavor triplet χ, namely, φ' and φ'', and the additional inert EW scalar doublets $\hat{\eta}$. In the following, we sketch the different production and decay channels and discuss their implications for direct searches at colliders as well as the current bounds on the existence of new particles beyond the SM. However, a detailed study is beyond the scope of this presentation.

After a brief discussion of electroweak precision constraints and a short summary of the main experimental results, we will discuss each class of new particles separately.

A. Electroweak precision constraints

The experimentally measured values of the oblique parameters S and T have been obtained by several precision measurements at large electron-positron (LEP) collider and Tevatron. The PDG [34] quotes values of $S = -0.04 \pm 0.09$ and $T = 0.07 \pm 0.08$ at 95% C.L. with a correlation between S and T of 88% for a reference value of $m_{h,\text{ref}} = 117$ GeV.

A general discussion in a multi-Higgs doublet model with an arbitrary number of Higgs doublets with hypercharge $Y = \pm\frac{1}{2}$ and an arbitrary number of SM singlets has been given in Ref. [62]. The expressions for the oblique parameters can be directly applied to this model, since the flavor symmetry only leads to additional restrictions on the masses and mixing matrices. We only estimate the contribution to S and T in the limit of small mixing in of $\hat{\eta}$, ϕ_i, H and only consider the mixing of φ' with φ'', which exactly corresponds to the region in parameter space being studied in the previous sections. In this limit also the charged and neutral scalar masses of the doublets $\hat{\eta}$ coincide. In this approximation, the contribution of H exactly cancels with the subtracted SM term, the contribution of $\hat{\eta}$ and ϕ_i to T vanishes, and ϕ_i does not contribute to S, since it does not couple to the gauge bosons in this approximation. Hence, the final contribution to S originates from $\hat{\eta}$ and is given by

$$S_{\eta,\phi} = \frac{\cos^2(2\theta_W)}{24\pi}\sum_{a=1}^{n}\tilde{G}\left(\frac{m_Z^2}{m_a^2}\right), \quad (7.1)$$

where $a = 1, \ldots, n$ sums over the EW doublets contained in $\hat{\eta}$ with the charged scalar masses m_a and θ_W denotes the Weinberg angle. The function $\tilde{G}$ is defined by

$$\tilde{G}(x) = -\frac{16}{3} + \frac{16}{z} - 2\left(\frac{4-z}{z}\right)^{3/2}\arctan\left(\frac{\sqrt{z(4-z)}}{2-z}\right). \quad (7.2)$$

Its absolute value is monotonously decreasing for $z \to 0$ starting from $\tilde{G}(1) = -0.216$ to $\tilde{G}(0) = 0$. The contribution from $\varphi'^{(\prime)}$ to S and T is given by

$$T_{\varphi'^{(\prime)}} = \frac{1}{8\pi\sin\theta_W^2 m_W^2}\sum_{a=1}^{2}\sum_{b=1}^{2}|U_{\varphi,ba}|^2 F(m_a^2, \mu_b^2), \quad (7.3)$$

$$S_{\varphi'^{(\prime)}} = \frac{1}{24\pi}\sum_{a=1}^{2}\left[\cos^2(2\theta_W)\tilde{G}\left(\frac{m_Z^2}{m_a^2}\right) + 2\ln\frac{\mu_a^2}{m_a^2}\right], \quad (7.4)$$

[13]Here we assume that H_q does not give a leading order contribution to the Weinberg operator. Symmetries can always be adjusted in order for this to be the case. If H_q does give such a contribution there will be one more free physical phase in the neutrino mass matrix that cannot be rotated away.

where the mixing matrix in the neutral $\varphi^{\prime(\prime)}$ sector, U_φ, is defined in Eq. (2.7) and m_a (μ_b) denotes the charged (neutral) masses of the fields contained in $\varphi^{\prime(\prime)}$. The function F is defined by

$$F(x,y) = \begin{cases} \frac{x+y}{2} - \frac{xy}{x-y}\ln\frac{x}{y} & \text{if } x \neq y \\ 0 & \text{if } x = y. \end{cases} \tag{7.5}$$

The next-to-leading order corrections are suppressed by small mixing angles in the scalar sector. Hence, the model is consistent with electroweak precision tests in the phenomenologically interesting region, i.e., for small mixing in the scalar sector.

B. Summary of relevant experimental results from colliders

Recently, after the initial announcement of a SM-Higgs-like resonance by ATLAS [3] and CMS [5], which was mainly based on the diphoton as well as the $h \to ZZ^* \to 4l$ channel, several other channels have been measured or updated [4,6]. We will briefly summarize the current status. The current best fit values for the mass of the resonance are $126.0 \pm 0.4(\text{stat}) \pm 0.4(\text{sys})$ GeV by ATLAS [3,4] and $125.8 \pm 0.4(\text{stat}) \pm 0.4(\text{sys})$ GeV by CMS [6]. The results are usually reported in terms of the signal strength normalized to the SM prediction, i.e.,

$$R_X \equiv \frac{\sigma(pp \to h)\text{Br}(h \to X)}{\sigma(pp \to h_{\text{SM}})\text{Br}(h_{\text{SM}} \to X)}.$$

The two main channels are the decay into two photons and $h \to ZZ^* \to 4l$. While the $h \to ZZ^* \to 4l$ rate seems to agree with the SM prediction with $R_{ZZ} = 1.2 \pm 0.6$ for ATLAS [4] and $R_{ZZ} = 0.8^{+0.35}_{-0.28}$ for CMS [6], the $h \to \gamma\gamma$ rate seems to be enhanced with $R_{\gamma\gamma} = 1.8 \pm 0.5$ for ATLAS and $R_{\gamma\gamma} = 1.56 \pm 0.43$ for CMS. The remaining channels include $h \to WW^*$ with a signal strength of $R_{WW} = 1.4 \pm 0.6$ (ATLAS) and $R_{WW} = 0.74 \pm 0.25$ (CMS) and the two channels with decays into fermions $hV \to b\bar{b}V$ with a signal strength of $R_{b\bar{b}V} = -0.4 \pm 1.1$ (ATLAS) and $R_{b\bar{b}V} = 1.3^{+0.7}_{-0.6}$ (CMS) as well as $h \to \tau\tau$ with $R_{\tau\bar{\tau}jj} = 0.7 \pm 0.7$ (ATLAS) and $R_{\tau\bar{\tau}jj} = 0.72 \pm 0.52$ (CMS). All channels but the decay of the Higgs boson to two photons are in agreement with the SM prediction. The deviation in the diphoton channel is intriguing, as in the SM this decay proceeds via a loop diagram and is thus sensitive to new physics contributions. However, so far, the deviation is at the 1–2σ level [63–65], if the uncertainties are taken into account conservatively. Besides the discovery of a Higgs-like resonance, the LHC has put strong constraints on any physics beyond the SM.

Charged Higgs particles are constrained by searches at LEP and LHC. At LEP, charged Higgs particles $H^\pm$ are produced via a virtual Z^* in the s channel, i.e., $e^+e^- \to Z^* \to H^+H^-$, and studied via their decays into $\tau\nu_\tau$ as well as $\bar{c}s$ assuming their branching ratios add up to 1, i.e., $\text{Br}(H^+ \to \tau^+\nu_\tau) + \text{Br}(H^+ \to c\bar{s}) = 1$. This results in a bound of $m_{H^+} > 79.3$ GeV [34]. Independent of any assumptions on the branching ratio, the invisible Z decay leads to $m_{H^+} \gtrsim 45$ GeV [34]. CMS searched for charged Higgs particles [66], which are produced in top decays, $t \to H^+b$ and constrains their branching ratio $\text{Br}(t \to H^+b)$ to less than 2%–4% for charged Higgs masses between 80 and 160 GeV. Similarly, the search by the ATLAS experiment [67] yields bounds on the branching ratio $\text{Br}(t \to H^+b)$ of the order of 1%–5% for charged Higgs masses in the range between 90 and 160 GeV, assuming $\text{Br}(H^+ \to \tau^+\nu_\tau) = 1$.

C. EW Higgs doublet H

We will first consider the limit in which there is no mixing between the Higgs h and the flavons ϕ_i. In the limit of no mixing, the tree-level couplings of the Higgs h contained in the EW Higgs doublet H to gauge bosons are identical to the SM couplings. In addition, the flavor conserving tree-level couplings of the Higgs h to fermions also agree with the SM ones. Note that there might be small corrections, since quark mixing vanishes at leading order and the Higgs couplings conserve all flavor numbers separately. As there are no new colored particles and the coupling of the Higgs to $t\bar{t}$ is the same as in the SM, the loop-induced coupling of the Higgs h to gluons agrees with the SM one. In summary, the production of the Higgs h as well as all tree-level decay channels and the decay into gluons are exactly like those in the SM. The Higgs decay into two photons is the only decay channel that can show a significant deviation from the SM in this approximation. If any of the other new scalars were light enough, there would be additional tree-level Higgs decays into pairs of these scalars and such scenarios are therefore constrained. The decay $h \to S\bar{S}$, if kinematically allowed, is loop suppressed.

Mixing of the Higgs h with the flavons ϕ_i leads to a suppression of all tree-level couplings to gauge bosons and fermions. Hence, the production cross section is reduced according to the admixture of the flavons ϕ_i to the Higgs boson. As Higgs decays into ZZ^* are close to the SM value, the admixture of the flavons ϕ_i to the Higgs h is limited.

Finally, let us discuss the diphoton decay channel. The SM contribution is dominated by the W boson contribution and the smaller top loop contribution, which interfere destructively. In our model, the decay into two photons receives additional contributions from charged scalars in the loop, which are contained in the EW doublets φ', φ'' as well as $\hat{\eta}$. Any enhancing contribution has to interfere constructively with the SM W boson loop or dominate over the W boson contribution. The contribution of

additional charged scalars ρ_i with a charge one, coupled to the Higgs boson via the Higgs portal

$$\mathcal{O}_{\rho_i} = c_{\rho_i} H^\dagger H |\rho_i|^2 \tag{7.6}$$

has recently been studied in Ref. [68]. The ratio of the effective coupling of the Higgs boson to two photons vs the SM prediction is given by

$$R_{\gamma\gamma} = \left| 1 - \sum_i c_{\rho_i} h(m_{\rho_i}) \right|^2, \tag{7.7}$$

where the function h is depicted in Fig. 10. To obtain an enhancement of a factor of 2 (1.5), one thus needs a value of

$$\sum_i c_{\rho_i} h(m_{\rho_i}) = \left\{ \begin{array}{ll} -0.41 \quad (-0.22) & \text{for constructive interference} \\ 2.41 \quad (2.22) & \text{for destructive interference} \end{array} \right\}. \tag{7.8}$$

Hence, a large negative coupling $c_\rho \sim -2$ is necessary to obtain an enhancement factor of 2 for a single singly charged scalar of mass 100 GeV. Such a large negative coupling destabilizes the vacuum and leads to charge breaking minima unless $|c_\rho| < \sqrt{\lambda \lambda_\rho} \sim \sqrt{\lambda_\rho}/2$ is fulfilled, where λ_ρ denotes the quartic coupling $\lambda_\rho |\rho|^4/2$. Note that this requires very large values for λ_ρ.

Let us now use this formula to estimate the deviations from $R_{\gamma\gamma} = 1$ that can be expected in this model. In total we have 11 charged scalars, 9 from the doublets $\hat{\eta}$ and 2 from the doublets φ', φ''. The interaction of the last two scalars with the Higgs field can be expressed as

$$c_{\varphi'} = \frac{m_h^2 + m_{\varphi'^+}^2}{v^2}, \qquad c_{\varphi''} = \frac{m_h^2 + m_{\varphi''^+}^2}{v^2}, \tag{7.9}$$

with $m^2_{\varphi'^{(\prime)+}}$ defined in Eq. (2.6). In the limit of large $m^2_{\varphi'^{(\prime)}}$ these two fields contribute

$$\begin{aligned} & c_{\varphi'} h(M_+^c) + c_{\varphi''} h(M_-^c) \\ & \quad = 0.1 + \left(\frac{22\ \text{GeV}}{M_+^c} \right)^2 + \left(\frac{22\ \text{GeV}}{M_-^c} \right)^2. \end{aligned} \tag{7.10}$$

The couplings of the charged components of the η fields are given by

$$\mathcal{O}_\eta = \sum_{i,J=1}^{3} c_{\eta_J} H^\dagger H |\eta_J^{(i)}|^2, \tag{7.11}$$

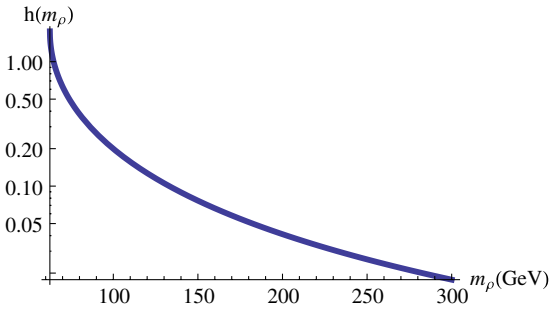

FIG. 10 (color online). Plot of function h of Eq. (7.8).

as dictated by the symmetry. The coefficients c_{η_J} are essentially unconstrained except for the fact that the combination that couples to the DM particle should not be too large, to avoid the bound from direct detection. In the limit where all charged scalars have a common mass M, we see from Fig. 11 that $M = 200$ GeV requires $\frac{1}{3}\sum_{J=1}^{3} c_{\eta_J} = -1.46\ (-0.95)$ for $R_{\gamma\gamma} = 2(1.5)$.

In case the $h \to \gamma\gamma$ anomaly persists, it would be interesting to measure $h \to \gamma Z$, since it originates from similar diagrams, where one photon is replaced by one Z boson. A cross correlation of the two measurements would allow one to determine the isospin of these particles. In our model all charged scalars are part of SU(2) doublets allowing us to distinguish it from other models which have EW multiplets in the loop with different EW charges, like singlets or triplets.

D. Further scalars

Besides the Higgs h, there are several additional scalars, such as the flavor-violating EW scalar doublets $\varphi'^{(\prime)}$ as well

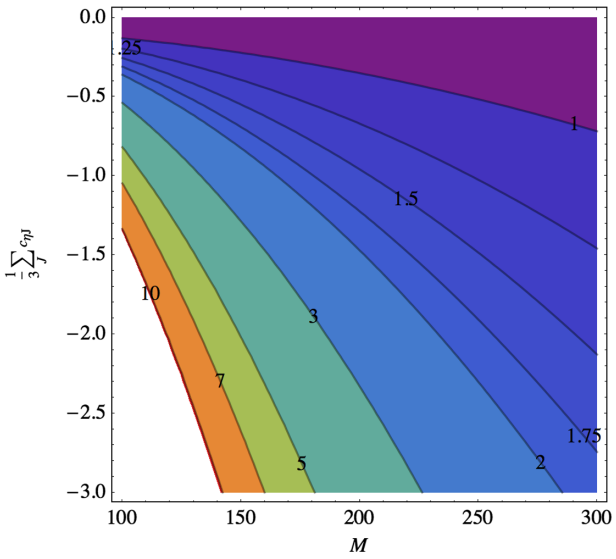

FIG. 11 (color online). $R_{\gamma\gamma}$ in the case where all charged scalars have the same common mass M as a function of $\frac{1}{3}\sum_{J=1}^{3} c_{\eta J}$.

as $\hat{\eta}$, which do not acquire a VEV, and the flavons ϕ_i, which acquire a VEV. See Appendix A for the scalar mass spectrum.

1. Flavor-violating Higgs doublets $\varphi^{\prime(\prime)}$

The neutral components of the flavor-violating Higgs doublets $\varphi^{\prime(\prime)}$ have neither tree-level couplings to $t\bar{t}$ nor couple to two EW gauge bosons at tree level. Hence, they are not produced by any of the standard Higgs production channels, but they can be produced via associate production with two different quarks, $gg \to \varphi^{\prime(\prime)} q q'$. The dominant channel is $gg \to \varphi' \bar{t} u$, $\varphi'' \bar{t} c$, which has a cross section of the same magnitude as production of a Higgs boson in association with a $t\bar{t}$ pair. Therefore, they are not constrained by the current heavy Higgs searches. Other production channels are $qq' \to \varphi^{\prime(\prime)}$, where q and q' are in different generations as well as pair production in vector boson fusion $WW, ZZ \to \varphi'\varphi', \varphi''\varphi''$. These processes are suppressed compared to the main Higgs production channels at the LHC. Note, however, that the decays of the flavor-violating Higgs doublets $\varphi^{\prime(\prime)}$ might lead to distinct flavor-violating signatures similar to the recent analyses of flavor-violating Higgs decays in models with flavor symmetries [25–28,69].

As the charged Higgs particles contained in $\varphi^{\prime(\prime)}$ do not couple to $t\bar{b}$, the LHC limits do not apply. Hence, the charged Higgs particles in our model are only constrained by the LEP limits discussed previously.

Although there are no constraints yet, upcoming searches will test the allowed range of masses, because the flavor-violating Higgs doublets $\varphi^{\prime(\prime)}$ stem from the same flavor triplet as the Higgs doublet H, and therefore their masses are determined to be given by scalar couplings times the EW VEV. Their masses may therefore not be raised arbitrarily high, as discussed below Eq. (2.6).[14]

2. EW scalar doublets $\hat{\eta}$

The neutral components of the EW scalar doublets $\hat{\eta}$ do not couple to quarks and particularly not to $t\bar{t}$ as well as two EW gauge bosons. They can be pair produced in vector boson fusion $WW, ZZ \to \eta_i \eta_i$. Hence, similarly to the flavor-violating Higgs doublets, they are not produced via the main Higgs production channels and the current bounds from heavy Higgs searches do not constrain $\hat{\eta}$. Also, the charged components of $\hat{\eta}$ are not constrained by the current LHC searches, because they do not couple to quarks directly and the charged Higgs bounds do not apply. Therefore, they are only constrained by the LEP searches.

3. Flavons ϕ_i

The flavons ϕ_i do not have gauge interactions and they do not couple to fermions directly. However, they mix with the Higgs h, which is constrained by the Higgs searches to be small, since a large mixing suppresses the production cross section of h and therefore all rates relative to the SM expectation. In conclusion, the scalar mass eigenstates that are dominantly composed of the flavons ϕ_i are only produced via mixing with the Higgs h, and thus there are no limits from current searches due to small mixing.

E. Variant with additional EW Higgs doublet H_q

As we discussed in Sec. VI, another simple possibility to incorporate quarks in the model is by assigning all quarks to the trivial representation of the flavor group and introducing an additional EW Higgs doublet H_q, which transforms trivially under the flavor group. This leads to different collider signatures compared to the previously discussed scenario. Soon, these scenarios can be experimentally distinguished at the LHC. We will highlight the most important differences.

The discussion of the fermions S as well as the scalars $\hat{\eta}$ remains the same. The main changes are in the Higgs phenomenology. In contrast to the other scenario, the component in χ which obtains a VEV does not couple to quarks and therefore it is not produced in gluon fusion, unless there is mixing between χ and H_q. Instead, the newly introduced Higgs H_q will be produced in gluon fusion. In this setup, the observed resonance at 125 GeV would be associated with the mass eigenstate, which is dominantly composed of Higgs H_q. As H_q has exactly the same couplings to gauge bosons and quarks, but does not couple to leptons (especially τ's), the decays into leptons are suppressed by the mixing between H_q and H (contained in χ). The diphoton branching ratio can be enhanced in the same way as discussed in Sec. VII C.

F. Fermionic singlets S

The additional fermionic states S are SM singlets and only charged under the discrete flavor group. Furthermore, they only couple to lepton doublets and therefore their production cross section at hadron colliders is suppressed compared to colored particles and there are no relevant analyses at present. The production depends on the exact mass spectrum of $\hat{\eta}$ as well as S. The production via the t-channel $\hat{\eta}$ exchange is always present in a lepton collider, e.g., $e^+e^- \to S\bar{S}$. If S is lighter than one of the components of $\hat{\eta}$, it is possible to produce S via EW production of these heavier components of $\hat{\eta}$ and subsequently decay into S and one lepton.

[14]Note that if one introduces soft-breaking terms that respect the Z_3 symmetry, it is possible to adjust the mass terms arbitrarily [22]. Alternatively one may introduce an EW singlet scalar that transforms as $\underline{\mathbf{3}}_\mathbf{1}$ and breaks to the same subgroup as χ. This can be realized without introducing a vacuum alignment problem.

Unless S is the DM candidate, the fermionic singlet S will decay into a lepton and one of the lighter components of $\hat{\eta}$, which will subsequently cascade down to DM via EW gauge interactions. The signal is missing transverse energy and leptons (and possibly EW gauge bosons) in the final state.

If S is lighter than all components of $\hat{\eta}$ and therefore a DM candidate, there are bounds from monophoton searches at LEP [70]. As S only couples to leptons, the searches at hadron colliders are weaker due to the additional suppression from loops that couple leptons to quarks. The monophoton searches at LEP probe the effective DM annihilation operator $(\bar{e}S)(e\bar{S})/\Lambda_t^2$, which are induced by the exchange of a scalar doublet $\eta_{1,2}$. The scale Λ_t of this operator is determined by $\Lambda_t^{-2} = \sum_k |h_k|^2/M_k^2$ for $M_k \gg M_S$. The analysis in Ref. [70] quotes a limit of (200–340) GeV for $M_S < 90$ GeV. Hence, this does not impose a strong constraint, since the smallness of neutrino masses points towards larger cutoff scales Λ_t.

VIII. CONCLUSIONS

We presented a predictive renormalizable A_4 model of lepton flavor at the electroweak scale. The flavor group A_4 is extended in the scalar potential to $Q_8 \rtimes A_4$, which allows a natural vacuum alignment at the EW scale [32]. This is the first model of its kind that explains the lepton flavor structure at the EW scale including the correct vacuum alignment.

The SM Higgs boson is subsumed in a flavor triplet that couples to charged leptons (and quarks) at the renormalizable level, thereby eliminating the need to invoke higher dimensional operators, as is done in models with flavon singlets. Neutrino masses are generated at the one-loop level and are further suppressed by the fact that two small mass insertions are needed in the loop. This TeV seesaw is realized without imposing any new symmetries apart from the flavor symmetries. In the model there are five real free parameters, which gives a predictive framework and, in particular, a correlation between the atmospheric and reactor angle is predicted, which agrees well with the recent global fits. Furthermore the model automatically includes a WIMP dark matter candidate and its stability and phenomenology have been studied. It can explain the observed dark matter abundance and is consistent with current exclusion limits by dark matter detection experiments. Constraints from LFV experiments are loosened by the flavor symmetry in comparison to flavor generic multi-Higgs doublet models due to the remnant Z_3 symmetry in the charged lepton sector.

Finally, several possible extensions to the quark sector have been studied. We studied the collider phenomenology of the simplest extension to the quark sector, which does not require the introduction of new particles at leading order and in which the quarks multiplets transform like the lepton multiplets under the flavor symmetry, and commented on the other possibilities. We studied the possibility of the Higgs boson h to explain the observed resonance at 125 GeV, especially the enhanced diphoton rate, which can be straightforwardly explained by the multitude of additional charged particles contained in the EW scalar doublets, which all contribute to the radiative decay of $h \to \gamma\gamma$. The fact that the Higgs doublet is contained in a flavor triplet leads to distinct signatures at the LHC. There are additional EW scalar doublets $\varphi'^{(\prime)}$, which cannot be decoupled from the Higgs h, and therefore are accessible in searches at the LHC. As they do not acquire a VEV, they do not decay into gauge bosons, but only via Yukawa type interactions into fermions besides decays into other scalars. Because of the remnant Z_3 flavor symmetry in the charged lepton sector, they only exhibit flavor violating decays into fermions in contrast to the Higgs h.

It might be interesting to study leptogenesis in this model. Because of the flavor symmetry, the fermionic SM singlet S are degenerate in mass at tree level as well as all couplings but λ_2 are real. The degeneracy is only lifted at two-loop order and therefore the induced mass splittings are small and there might be a resonant enhancement. This also introduces some CP violation into the mass matrix of S, but it has to be checked whether it is sufficient. We will leave a study of possible ways to obtain the baryon asymmetry of the Universe for future work.

ACKNOWLEDGMENTS

M. H. acknowledges support by the International Max Planck Research School for Precision Tests of Fundamental Symmetries. M. L. and M. S. thank the Galileo Galilei Institute for Theoretical Physics for its hospitality. M. S. would like to thank K. Petraki for discussions and would like to acknowledge MPI für Kernphysik, where part of this work was done, for hospitality of its staff and the generous support. This work was supported in part by the Australian Research Council.

APPENDIX A: VACUUM ALIGNMENT AND SCALAR SPECTRUM OF

1. Vacuum alignment

The vacuum configuration given in Eq. (2.1) is naturally obtained from the most general potential[15]

$$V = V_\phi(\phi_1, \phi_2) + V_\chi(\chi) + V_{\text{mix}}(\chi, \phi_1, \phi_2)$$

compatible with given symmetries, where $V_\chi(\chi)$ is given in (2.4) and

[15]We do not have to consider the part involving $\hat{\eta}$, because it does not change the minimization conditions of ϕ_i and χ, if it does not acquire a VEV.

$$
\begin{aligned}
V_\phi(\phi_1,\phi_2) &= \mu_1^2(\phi_1\phi_1)_{\underline{\mathbf{1}}_1} + \alpha_1(\phi_1\phi_1)^2_{\underline{\mathbf{1}}_1} + \sum_{i=2,3}\alpha_i(\phi_1\phi_1)_{\underline{\mathbf{3}}_i}\cdot(\phi_1\phi_1)_{\underline{\mathbf{3}}_i} + \mu_2^2(\phi_2\phi_2)_{\underline{\mathbf{1}}_1} + \beta_1(\phi_2\phi_2)^2_{\underline{\mathbf{1}}_1} \\
&\quad + \sum_{i=2,3}\beta_i(\phi_2\phi_2)_{\underline{\mathbf{3}}_i}\cdot(\phi_2\phi_2)_{\underline{\mathbf{3}}_i} + \gamma_1(\phi_1\phi_1)_{\underline{\mathbf{1}}_1}(\phi_2\phi_2)_{\underline{\mathbf{1}}_1} + \sum_{i=2,3,4}\gamma_i(\phi_1\phi_1)_{\underline{\mathbf{3}}_i}\cdot(\phi_2\phi_2)_{\underline{\mathbf{3}}_i}, \\
V_\chi(\chi) &= \mu_3^2(\chi\chi)_{\underline{\mathbf{1}}_1} + \rho_1(\chi\chi\chi)_{\underline{\mathbf{1}}_1} + \lambda_1(\chi\chi)^2_{\underline{\mathbf{1}}_1} + \lambda_2(\chi\chi)_{\underline{\mathbf{1}}_2}(\chi\chi)_{\underline{\mathbf{1}}_3}, \\
V_{\mathrm{mix}}(\chi,\phi_1,\phi_2) &= \zeta_{13}(\phi_1\phi_1)_{\underline{\mathbf{1}}_1}(\chi^\dagger\chi)_{\underline{\mathbf{1}}_1} + \zeta_{23}(\phi_2\phi_2)_{\underline{\mathbf{1}}_1}(\chi^\dagger\chi)_{\underline{\mathbf{1}}_1}
\end{aligned}
\tag{A1}
$$

is compatible with given symmetries. The minimization conditions reduce to the equations

$$
\begin{aligned}
a(\alpha_+(a^2+b^2)+\alpha_-(a^2-b^2)+\gamma_+(c^2+d^2)+\gamma_-(c^2-d^2)+U_1)+\Gamma bcd &= 0, \\
b(\alpha_+(a^2+b^2)-\alpha_-(a^2-b^2)+\gamma_+(c^2+d^2)-\gamma_-(c^2-d^2)+U_1)+\Gamma acd &= 0, \\
c(\beta_+(c^2+d^2)+\beta_-(c^2-d^2)+\gamma_+(a^2+b^2)+\gamma_-(a^2-b^2)+U_2)+\Gamma abd &= 0, \\
d(\beta_+(c^2+d^2)-\beta_-(c^2-d^2)+\gamma_+(a^2+b^2)-\gamma_-(a^2-b^2)+U_2)+\Gamma abc &= 0, \\
v(M_\chi^2+\lambda_\chi v^2) &= 0,
\end{aligned}
\tag{A2}
$$

with

$$
U_i = \frac{1}{2}\mu_i^2 + \frac{\sqrt{3}}{12}\zeta_{i3}v^2 \quad \text{for} \quad i=1,2,
$$

and

$$
M_\chi^2 = 2\mu_3^2 + \zeta_{13}(a^2+b^2) + \zeta_{23}(c^2+d^2), \qquad \lambda_\chi = \frac{2}{3}(\sqrt{3}\lambda_{\chi\underline{\mathbf{1}}_1} + \lambda_{\chi\underline{\mathbf{3}}_{1S}}),
$$

$$
\xi_+ = \frac{\xi_1}{2}, \qquad \xi_- = \frac{\xi_2+\xi_3}{2\sqrt{3}}, \qquad \gamma_+ = \frac{\sqrt{3}\gamma_1+\gamma_4}{4\sqrt{3}}, \qquad \gamma_- = \frac{\gamma_2+\gamma_3}{4\sqrt{3}}, \quad \text{and} \quad \Gamma = \frac{\gamma_4}{\sqrt{3}},
$$

with $\xi = \alpha,\ \beta$. Since the number of equations matches the number of VEVs, vacuum alignment is possible. Corrections to the scalar potential only arise on dimension six level. These corrections furthermore arise on one-loop level and are thus further suppressed. We therefore neglect VEV shifts arising from these interactions throughout this work.

2. Scalar spectrum ϕ_i, χ

Let us first discuss the visible sector, i.e., the flavons ϕ_1, ϕ_2, χ that get VEVs and realize the symmetry breaking; the η's are independent and will be discussed later. The fields can be classified according to remnant symmetries of the potential. There are the obvious symmetries

$$
Z_3\colon \chi \to T_3\chi, \qquad \phi_i \to \phi_i, \tag{A3}
$$

with $T_3 = \Omega_T \mathrm{diag}(1,\omega^2,\omega)\Omega_T^\dagger$ and

$$
Z_2\colon \phi_i \to S_4\phi_i, \qquad \chi \to \chi, \tag{A4}
$$

with $S_4 = \Omega_{S_4}\mathrm{diag}(1,1,-1,-1)\Omega_{S_4}^\dagger$ but there is another accidental symmetry of the potential V_ϕ not part of $Q_8 \rtimes A_4$:

$$
Z_2\colon \phi_i \to O_4\phi_i, \qquad \chi \to \chi, \tag{A5}
$$

with[16] $O_4 = \Omega_{S_4}\mathrm{diag}(1,1,1,-1)\Omega_{S_4}^\dagger$, where

$$
\Omega_{S_4} \equiv \frac{1}{\sqrt{2}}\begin{pmatrix} 0 & 1 & 0 & -1 \\ 0 & 1 & 0 & 1 \\ -1 & 0 & 1 & 0 \\ 1 & 0 & 1 & 0 \end{pmatrix}. \tag{A6}
$$

It is useful to go to a basis

$$
\begin{aligned}
\tilde{\phi}_i &= \Omega_{S_4}^\dagger\phi_i, \\
(H,\varphi',\varphi'')^T &= \Omega_T^\dagger\chi, \\
(L_e,L_\mu,L_\tau)^T &= \Omega_T^\dagger L,
\end{aligned}
\tag{A7}
$$

where these symmetries are represented diagonally. Let us discuss the mass terms in turn:

(i) The nine physical scalars contained in χ have been discussed following Eq. (2.6). Here we only report the expressions of the dimensionless couplings in terms of masses:

[16]The alert reader will recognize this as an outer automorphism h_4 defined in Ref. [71].

$$\begin{aligned}
\lambda_{\chi^{1}_{1}} &= M_{-}^{2} + M_{+}^{2} + \frac{3m_h^2}{2},\\
\lambda_{\chi^{1}_{2}} &= \frac{1}{2}\left(3m_1^2 - 3\sqrt{m_1^4 - 2m_1^2m_2^2 + m_2^4 - 4(M_{-}^{2} - M_{+}^{2})^2} + 3m_2^2 - 2M_{-}^{2} - 2M_{+}^{2}\right),\\
\lambda_{\chi^{3}_{1},S} &= -\sqrt{3}(M_{-}^{2} + M_{+}^{2}),\\
\lambda_{\chi^{3}_{1},A} &= -\sqrt{3}\left(m_1^2 + \sqrt{m_1^4 - 2m_1^2m_2^2 + m_2^4 - 4(M_{-}^{2} - M_{+}^{2})^2} + m_2^2 - M_{-}^{2} - M_{+}^{2}\right),\\
\lambda_{\chi A} &= 6(M_{-}^{2} - M_{+}^{2}).
\end{aligned} \tag{A8}$$

(ii) $(\tilde{\phi}_1)_4$ and $(\tilde{\phi}_2)_4$ transform as $(1, -1, -1)$ and have a mass matrix given by

$$\begin{pmatrix} m_{11} & \frac{2(ac(\sqrt{3}\gamma_M - 2\gamma_2) + 2b\gamma_2 d)}{\sqrt{3}} \\ . & m_{11}((a,b,c,d,\alpha_2) \leftrightarrow (c,d,a,b,\beta_2)) \end{pmatrix}$$

with

$$m_{11} = -4\sqrt{3}a^2\alpha_2 + a\left(\frac{2a\gamma_M(c-d)(c+d)}{(b-a)(a+b)} + \frac{c\Gamma d}{b}\right) - \frac{bc\Gamma d}{2a} + \frac{1}{12}(48\sqrt{3}\alpha_2 b^2 - 3\Gamma(c^2+d^2) + 8\sqrt{3}\gamma_2(d^2-c^2)).$$

(iii) $(\tilde{\phi}_1)_3$ and $(\tilde{\phi}_2)_3$ transform as $(1, -1, 1)$ and have a mass matrix given by

$$\begin{pmatrix} m_{11} & \frac{2(ac\gamma_2 - bd(\gamma_2 - 2\sqrt{3}\gamma_M))}{\sqrt{3}} \\ . & m_{11}((a,b,c,d,\alpha_2) \leftrightarrow (c,d,a,b,\beta_2)) \end{pmatrix}$$

with

$$\begin{aligned}
m_{11} = {} & 2\sqrt{3}a^2\alpha_2 + \frac{2b^2(\sqrt{3}\alpha_2(a-b)(a+b) + 2\gamma_M(c-d)(c+d))}{b^2 - a^2} - \frac{ac\Gamma d}{b} + \frac{2bc\Gamma d}{a}\\
& - \frac{1}{2}\Gamma(c^2+d^2) + \frac{\gamma_2(c-d)(c+d)}{\sqrt{3}}.
\end{aligned}$$

(iv) The real scalars h, $(\tilde{\phi}_1)_1$, $(\tilde{\phi}_1)_2$, $(\tilde{\phi}_2)_1$, and $(\tilde{\phi}_2)_2$ transform as $(1, 1, 1)$ under the remnant symmetry. Here we do not give the full mass matrix but only give the mixing with the Higgs boson in the limit of small mixings. The mixing matrix with field f is given by

$$\tan 2\theta_f = \frac{2m_{h,f}}{m_f^2 - m_h^2} \tag{A9}$$

with

$$m_{h,(\tilde{\phi}_1)_1} = -\frac{bv\zeta_{13}}{\sqrt{3}}, \qquad m_{h,(\tilde{\phi}_1)_2} = \frac{av\zeta_{13}}{\sqrt{3}}, \qquad m_{h,(\tilde{\phi}_2)_1} = -\frac{dv\zeta_{23}}{\sqrt{3}}, \qquad m_{h,(\tilde{\phi}_2)_2} = \frac{cv\zeta_{23}}{\sqrt{3}}.$$

3. Scalar spectrum—$\hat{\eta}$

The relevant part of the scalar potential to calculate the mass insertions needed to calculate neutrino masses for the mass spectrum of $\hat{\eta}$ has been given in Eqs. (3.5), (3.6), (3.7), and (3.8). To calculate the η mass spectrum the complete interactions

TABLE II. Representations of $Q_8 \rtimes A_4$ in the chosen basis. The first 4 representations are the unfaithful $A_4 = \langle S, T \rangle$ representations to which the leptons are assigned (with $\rho(X) = \mathbb{1}$). Note that the representations $\underline{\mathbf{4}}_\mathbf{i}$ are double valued, i.e., $\rho(Z(G) = X^2) = -\mathbb{1}$, whereas the other representations are single valued ($\rho(X^2) = \mathbb{1}$). $\underline{\mathbf{1}}_{\mathbf{2,3}}$ and $\underline{\mathbf{4}}_{\mathbf{2,3}}$ are complex, the other representations are real.

	$\underline{\mathbf{1}}_\mathbf{1}$	$\underline{\mathbf{1}}_\mathbf{2}$	$\underline{\mathbf{1}}_\mathbf{3}$	$\underline{\mathbf{3}}_\mathbf{1}$	$\underline{\mathbf{3}}_\mathbf{2}$	$\underline{\mathbf{3}}_\mathbf{3}$	$\underline{\mathbf{3}}_\mathbf{4}$	$\underline{\mathbf{3}}_\mathbf{5}$	$\underline{\mathbf{4}}_\mathbf{1}$	$\underline{\mathbf{4}}_\mathbf{2}$	$\underline{\mathbf{4}}_\mathbf{3}$
S	1	1	1	S_3	$T_3 S_3 T_3^2$	$T_3 S_3 T_3^2$	$\mathbb{1}_3$	$T_3^2 S_3 T_3$	S_4	S_4	S_4
T	1	ω	ω^2	T_3	T_3	T_3	T_3	T_3	T_4	$\omega^2 T_4$	ωT_4
X	1	1	1	$\mathbb{1}_3$	S_3	$T_3^2 S_3 T_3$	$T_3 S_3 T_3^2$	$T_3^2 S_3 T_3$	X_4	X_4	X_4

$$
\begin{aligned}
\delta V_{\hat{\eta}}^{(2)} = {} & \lambda_1 (\chi^T \sigma_2 \vec{\sigma} \chi)_{\underline{\mathbf{1}}_\mathbf{1}} (\eta_1^T \sigma_2 \vec{\sigma} \eta_3)^*_{\underline{\mathbf{1}}_\mathbf{1}} + \lambda_2 e^{i\alpha_\lambda} (\chi^T \sigma_2 \vec{\sigma} \chi)_{\underline{\mathbf{3}}_\mathbf{1}} (\eta_2^T \sigma_2 \vec{\sigma} \eta_3)^*_{\underline{\mathbf{3}}_\mathbf{1}} + \lambda_3 (\phi_1 \phi_2)_{\underline{\mathbf{1}}_\mathbf{1}} (\eta_3^\dagger \eta_1)_{\underline{\mathbf{1}}_\mathbf{1}} \\
& + \lambda_4 (\phi_1 \phi_2)_{\underline{\mathbf{3}}_\mathbf{1}} (\eta_3^\dagger \eta_2)_{\underline{\mathbf{3}}_\mathbf{1}} + \lambda_5 (\phi_1 \phi_2)_{\underline{\mathbf{3}}_\mathbf{2}} (\eta_3^\dagger \eta_2)_{\underline{\mathbf{3}}_\mathbf{2}} + \lambda_6 (\phi_1 \phi_2)_{\underline{\mathbf{3}}_\mathbf{3}} (\eta_3^\dagger \eta_2)_{\underline{\mathbf{3}}_\mathbf{3}} + \lambda_7 (\phi_1 \phi_2)_{\underline{\mathbf{3}}_\mathbf{5}} (\eta_1^\dagger \eta_3)_{\underline{\mathbf{3}}_\mathbf{5S}} \\
& + \lambda_8 (\phi_1 \phi_2)_{\underline{\mathbf{3}}_\mathbf{5}} (\eta_1^\dagger \eta_3)_{\underline{\mathbf{3}}_\mathbf{5A}} + l_1^{ij} (\phi_j \phi_j)_{\underline{\mathbf{1}}_\mathbf{1}} (\eta_i^\dagger \eta_i)_{\underline{\mathbf{1}}_\mathbf{1}} + l_2^j (\phi_j \phi_j)_{\underline{\mathbf{3}}_{\mathbf{2,3}}} (\eta_1^\dagger \eta_2)_{\underline{\mathbf{3}}_{\mathbf{2,3}}} + l_3^j (\phi_j \phi_j)_{\underline{\mathbf{3}}_\mathbf{4}} (\eta_2^\dagger \eta_2)_{\underline{\mathbf{3}}_\mathbf{4}} \\
& + k_1 (\chi^\dagger \chi)_{\underline{\mathbf{3}}_\mathbf{1}} (\eta_1^\dagger \eta_2)_{\underline{\mathbf{3}}_\mathbf{1}} + k_2 (\chi^\dagger \sigma_2 \vec{\sigma} \chi)_{\underline{\mathbf{3}}_\mathbf{1}} (\eta_1^\dagger \sigma_2 \vec{\sigma} \eta_2)_{\underline{\mathbf{3}}_\mathbf{1}} + k_3^{(i)} (\chi^\dagger \sigma_2 \vec{\sigma} \chi)_{\underline{\mathbf{1}}_\mathbf{1}} (\eta_i^\dagger \sigma_2 \vec{\sigma} \eta_i)_{\underline{\mathbf{1}}_\mathbf{1}} \\
& + k_4^{(i)} (\chi^\dagger \chi)_{\underline{\mathbf{1}}_\mathbf{1}} (\eta_i^\dagger \eta_i)_{\underline{\mathbf{1}}_\mathbf{1}} + \text{H.c.}
\end{aligned} \tag{A10}
$$

are needed. Let us briefly outline how the various couplings act: The couplings $k_4^{(i)}$ and $l_1^{(ij)}$ renormalize M_i, $k_3^{(i)}$ splits masses of charged and neutral components, and λ_1 and λ_2 mix neutral scalar and pseudoscalar components of the various fields. Hence, it also splits the masses of scalar and pseudoscalar of the lightest mass eigenstate, and k_1, $l_2^{(i)}$, $l_3^{(j)}$ mix the components of the various $\hat{\eta}$ and adds flavor breaking effects. Since $\langle \chi^2_{\underline{\mathbf{1}}_{\mathbf{2,3}}} \rangle = 0$ such couplings do give contributions to mass terms and are not shown here. $\lambda_3, \ldots, \lambda_8$ break Z_4 and therefore mix components of η_3 with components of $\eta_{1,2}$.

APPENDIX B: GROUP THEORY

In this section, we give a short review of the relevant group theory of $Q_8 \rtimes A_4$. We give the presentation of the group and a possible set of generators for all irreducible representations of the group. We summarize the most important Clebsch-Gordan coefficients for the quartet $\underline{\mathbf{4}}_\mathbf{1}$ and triplets $\underline{\mathbf{3}}_\mathbf{i}$. See Ref. [32] for a more detailed description of the group theory of $Q_8 \rtimes A_4$. All Clebsch-Gordan coefficients can be obtained with the help of the Mathematica package DISCRETE, which has been published as part of Ref. [32].

1. Mini review

The semidirect product $Q_8 \rtimes A_4$ we are using is defined by the relations

$$
\begin{aligned}
SXS^{-1} &= X, & SYS^{-1} &= Y^{-1}, \\
TXT^{-1} &= YX, & TYT^{-1} &= X,
\end{aligned} \tag{B1}
$$

between the generators of A_4

$$
\langle S, T | S^2 = T^3 = (ST)^3 = 1 \rangle, \tag{B2}
$$

and Q_8

$$
\langle X, Y | X^4 = 1, X^2 = Y^2, Y^{-1} X Y = X^{-1} \rangle. \tag{B3}
$$

Note that it is sufficient to use e.g., the generators X, S, T as $Y = T^{-1} X T$. The defining representation matrices for the representations we are using are given in Table II with

$$
\begin{aligned}
S_3 &= \begin{pmatrix} 1 & 0 & 0 \\ 0 & -1 & 0 \\ 0 & 0 & -1 \end{pmatrix}, \qquad T_3 = \begin{pmatrix} 0 & 1 & 0 \\ 0 & 0 & 1 \\ 1 & 0 & 0 \end{pmatrix}, \\
T_4 &= \begin{pmatrix} 0 & 1 & 0 & 0 \\ 0 & 0 & 1 & 0 \\ 1 & 0 & 0 & 0 \\ 0 & 0 & 0 & 1 \end{pmatrix},
\end{aligned} \tag{B4}
$$

and $S_4 = \sigma_3 \otimes \sigma_1$ and $X_4 = -i\sigma_2 \otimes \sigma_3$.

2. Clebsch-Gordan coefficients: Quartets

The most important Clebsch-Gordan coefficients for the quartets $a, b \sim \underline{\mathbf{4}}_\mathbf{1}$ are given by

$$
(a^\dagger b)_{\underline{\mathbf{1}}_\mathbf{1}} = \frac{1}{2} (a_1^\dagger b_1 + a_2^\dagger b_2 + a_3^\dagger b_3 + a_4^\dagger b_4) \tag{B5}
$$

and the triplets

$$(a^\dagger b)_{\underline{\mathbf{3}}_1} = \frac{1}{2}\begin{pmatrix} -a_4^\dagger b_1 + a_3^\dagger b_2 - a_2^\dagger b_3 + a_1^\dagger b_4 \\ -a_3^\dagger b_1 - a_4^\dagger b_2 + a_1^\dagger b_3 + a_2^\dagger b_4 \\ a_2^\dagger b_1 - a_1^\dagger b_2 - a_4^\dagger b_3 + a_3^\dagger b_4 \end{pmatrix}, \qquad (a^\dagger b)_{\underline{\mathbf{3}}_2} = \frac{1}{2}\begin{pmatrix} a_4^\dagger b_1 + a_3^\dagger b_2 + a_2^\dagger b_3 + a_1^\dagger b_4 \\ a_3^\dagger b_1 + a_4^\dagger b_2 + a_1^\dagger b_3 + a_2^\dagger b_4 \\ a_2^\dagger b_1 + a_1^\dagger b_2 + a_4^\dagger b_3 + a_3^\dagger b_4 \end{pmatrix},$$
$$(a^\dagger b)_{\underline{\mathbf{3}}_3} = \frac{1}{2}\begin{pmatrix} a_1^\dagger b_1 - a_2^\dagger b_2 - a_3^\dagger b_3 + a_4^\dagger b_4 \\ -a_1^\dagger b_1 + a_2^\dagger b_2 - a_3^\dagger b_3 + a_4^\dagger b_4 \\ -a_1^\dagger b_1 - a_2^\dagger b_2 + a_3^\dagger b_3 + a_4^\dagger b_4 \end{pmatrix}, \qquad (a^\dagger b)_{\underline{\mathbf{3}}_4} = \frac{1}{2}\begin{pmatrix} a_4^\dagger b_1 - a_3^\dagger b_2 - a_2^\dagger b_3 + a_1^\dagger b_4 \\ -a_3^\dagger b_1 + a_4^\dagger b_2 - a_1^\dagger b_3 + a_2^\dagger b_4 \\ -a_2^\dagger b_1 - a_1^\dagger b_2 + a_4^\dagger b_3 + a_3^\dagger b_4 \end{pmatrix}, \qquad \text{(B6)}$$
$$(a^\dagger b)_{\underline{\mathbf{3}}_5} = \frac{1}{2}\begin{pmatrix} -a_4^\dagger b_1 - a_3^\dagger b_2 + a_2^\dagger b_3 + a_1^\dagger b_4 \\ a_3^\dagger b_1 - a_4^\dagger b_2 - a_1^\dagger b_3 + a_2^\dagger b_4 \\ -a_2^\dagger b_1 + a_1^\dagger b_2 - a_4^\dagger b_3 + a_3^\dagger b_4 \end{pmatrix}.$$

Note that $[(a^\dagger b)_{\underline{\mathbf{3}}_i}]^* = (b^\dagger a)_{\underline{\mathbf{3}}_i}$ is real for $i = 2, 3, 4$ and $[(a^\dagger b)_{\underline{\mathbf{3}}_i}]^* = -(b^\dagger a)_{\underline{\mathbf{3}}_i}$ for $i = 1, 5$.

3. Clebsch-Gordan coefficients: Triplets

Furthermore, the most important Clebsch-Gordan coefficients for the three-dimensional representations $\underline{\mathbf{3}}_\mathbf{i}$ are described by

$$(a^\dagger b)_{\underline{\mathbf{1}}_1} = \frac{1}{\sqrt{3}}(a_1^\dagger b_1 + a_2^\dagger b_2 + a_3^\dagger b_3),$$
$$(a^\dagger b)_{\underline{\mathbf{1}}_2} = \frac{1}{\sqrt{3}}(a_1^\dagger b_1 + \omega^2 a_2^\dagger b_2 + \omega a_3^\dagger b_3), \qquad (a^\dagger b)_{\underline{\mathbf{1}}_3} = \frac{1}{\sqrt{3}}(a_1^\dagger b_1 + \omega a_2^\dagger b_2 + \omega^2 a_3^\dagger b_3), \qquad \text{(B7)}$$
$$(a^\dagger b)_{A,\underline{\mathbf{3}}} = \frac{1}{2}\begin{pmatrix} a_2^\dagger b_3 - a_3^\dagger b_2 \\ a_3^\dagger b_1 - a_1^\dagger b_3 \\ a_1^\dagger b_2 - a_2^\dagger b_1 \end{pmatrix}, \qquad (a^\dagger b)_{S,\underline{\mathbf{3}}} = \frac{1}{2}\begin{pmatrix} a_2^\dagger b_3 + a_3^\dagger b_2 \\ a_3^\dagger b_1 + a_1^\dagger b_3 \\ a_1^\dagger b_2 + a_2^\dagger b_1 \end{pmatrix},$$

where (a_1, a_2, a_3), $(b_1, b_2, b_3) \sim \underline{\mathbf{3}}$. Note that $(a^\dagger a)_{A,\underline{\mathbf{3}}}$ is imaginary and $(a^\dagger a)_{S,\underline{\mathbf{3}}}$ is real. Other important products are the product of $a \sim \underline{\mathbf{3}}_\mathbf{5}$ and $b \sim \underline{\mathbf{3}}_\mathbf{4}$:

$$(a^\dagger b)_{\underline{\mathbf{3}}_1} = \begin{pmatrix} a_2^\dagger b_3 \\ a_3^\dagger b_1 \\ a_1^\dagger b_2 \end{pmatrix}, \qquad (a^\dagger b)_{\underline{\mathbf{3}}_2} = \begin{pmatrix} a_3^\dagger b_2 \\ a_1^\dagger b_3 \\ a_2^\dagger b_1 \end{pmatrix}, \qquad (a^\dagger b)_{\underline{\mathbf{3}}_3} = \begin{pmatrix} a_3^\dagger b_3 \\ a_1^\dagger b_1 \\ a_2^\dagger b_2 \end{pmatrix}, \qquad \text{(B8)}$$

of $a \sim \underline{\mathbf{3}}_\mathbf{5}$ and $b \sim \underline{\mathbf{3}}_\mathbf{2}$

$$(a^\dagger b)_{\underline{\mathbf{3}}_1} = \begin{pmatrix} a_3^\dagger b_2 \\ a_1^\dagger b_3 \\ a_2^\dagger b_1 \end{pmatrix}, \qquad (a^\dagger b)_{\underline{\mathbf{3}}_3} = \begin{pmatrix} a_2^\dagger b_2 \\ a_3^\dagger b_3 \\ a_1^\dagger b_1 \end{pmatrix}, \qquad (a^\dagger b)_{\underline{\mathbf{3}}_4} = \begin{pmatrix} a_2^\dagger b_3 \\ a_3^\dagger b_1 \\ a_1^\dagger b_2 \end{pmatrix}, \qquad \text{(B9)}$$

and of $a \sim \underline{\mathbf{3}}_\mathbf{4}$ and $b \sim \underline{\mathbf{3}}_\mathbf{2}$

$$(a^\dagger b)_{\underline{\mathbf{3}}_1} = \begin{pmatrix} a_2^\dagger b_3 \\ a_3^\dagger b_1 \\ a_1^\dagger b_2 \end{pmatrix}, \qquad (a^\dagger b)_{\underline{\mathbf{3}}_3} = \begin{pmatrix} a_1^\dagger b_1 \\ a_2^\dagger b_2 \\ a_3^\dagger b_3 \end{pmatrix}, \qquad (a^\dagger b)_{\underline{\mathbf{3}}_5} = \begin{pmatrix} a_3^\dagger b_2 \\ a_1^\dagger b_3 \\ a_2^\dagger b_1 \end{pmatrix}. \qquad \text{(B10)}$$

[1] F. An *et al.* (DAYA-BAY Collaboration), Phys. Rev. Lett. **108**, 171803 (2012); J. Ahn *et al.* (RENO Collaboration), Phys. Rev. Lett. **108**, 191802 (2012).

[2] K. Abe *et al.*, Phys. Rev. Lett. **107**, 041801 (2011); P. Adamson *et al.* (MINOS Collaboration), Phys. Rev. Lett. **107**, 181802 (2011); Y. Abe *et al.* (DOUBLE-CHOOZ Collaboration), Phys. Rev. Lett. **108**, 131801 (2012).

[3] G. Aad *et al.*, Phys. Lett. B **716**, 1 (2012).

[4] CERN, Geneva, Technical Report No. ATLAS-CONF-2012-162, 2012.

[5] S. Chatrchyan *et al.*, Phys. Lett. B **716**, 30 (2012).

[6] CERN, Geneva, Technical Report No. CMS-HIG-12-045, 2012.

[7] D. Forero, M. Tortola, and J. Valle, Phys. Rev. D **86**, 073012 (2012).

[8] G. L. Fogli, E. Lisi, A. Marrone, D. Montanino, A. Palazzo, and A. M. Rotunno, Phys. Rev. D **86**, 013012 (2012); M. Gonzalez-Garcia, M. Maltoni, J. Salvado, and T. Schwetz, arXiv:1209.3023.

[9] A. de Gouvea and H. Murayama, arXiv:1204.1249.

[10] A. de Gouvea and H. Murayama, Phys. Lett. B **573**, 94 (2003).

[11] L. J. Hall, H. Murayama, and N. Weiner, Phys. Rev. Lett. **84**, 2572 (2000).

[12] J. Espinosa, arXiv:hep-ph/0306019.

[13] G. Altarelli, F. Feruglio, I. Masina, and L. Merlo, J. High Energy Phys. 11 (2012) 139.

[14] R. de Adelhart Toorop, F. Feruglio, and C. Hagedorn, Nucl. Phys. **B858**, 437 (2012).

[15] G.-J. Ding, Nucl. Phys. **B862**, 1 (2012).

[16] S. F. King, C. Luhn, and A. J. Stuart, Nucl. Phys. **B867**, 203 (2013).

[17] E. Ma and G. Rajasekaran, Phys. Rev. D **64**, 113012 (2001).

[18] E. Ma, Phys. Rev. D **73**, 077301 (2006).

[19] J. Kubo, E. Ma, and D. Suematsu, Phys. Lett. B **642**, 18 (2006).

[20] M. Hirsch, S. Morisi, and J. Valle, Phys. Lett. B **679**, 454 (2009).

[21] D. Ibanez, S. Morisi, and J. Valle, Phys. Rev. D **80**, 053015 (2009).

[22] E. Ma, Phys. Rev. D **82**, 037301 (2010).

[23] R. de Adelhart Toorop, F. Bazzocchi, L. Merlo, and A. Paris, J. High Energy Phys. 03 (2011) 035.

[24] R. de Adelhart Toorop, F. Bazzocchi, L. Merlo, and A. Paris, J. High Energy Phys. 03 (2011) 040.

[25] G. Bhattacharyya, P. Leser, and H. Pas, Phys. Rev. D **83**, 011701 (2011).

[26] Q.-H. Cao, A. Damanik, E. Ma, and D. Wegman, Phys. Rev. D **83**, 093012 (2011).

[27] Q.-H. Cao, S. Khalil, E. Ma, and H. Okada, Phys. Rev. Lett. **106**, 131801 (2011).

[28] G. Bhattacharyya, P. Leser, and H. Pas, Phys. Rev. D **86**, 036009 (2012); G. Bhattacharyya, I. de Medeiros Varzielas, and P. Leser, Phys. Rev. Lett. **109**, 241603 (2012).

[29] K. Babu, E. Ma, and J. Valle, Phys. Lett. B **552**, 207 (2003); E. Ma, Phys. Rev. D **70**, 031901 (2004); G. Altarelli and F. Feruglio, Nucl. Phys. **B720**, 64 (2005); K. Babu and X.-G. He, arXiv:hep-ph/0507217; G. Altarelli and F. Feruglio, Nucl. Phys. **B741**, 215 (2006); X.-G. He, Y.-Y. Keum, and R. R. Volkas, J. High Energy Phys. 04 (2006) 039.

[30] B. Brahmachari, S. Choubey, and M. Mitra, Phys. Rev. D **77**, 073008 (2008); E. Ma and D. Wegman, Phys. Rev. Lett. **107**, 061803 (2011); Y. Shimizu, M. Tanimoto, and A. Watanabe, Prog. Theor. Phys. **126**, 81 (2011); S. F. King and C. Luhn, J. High Energy Phys. 09 (2011) 042; S. Antusch, S. F. King, C. Luhn, and M. Spinrath, Nucl. Phys. **B856**, 328 (2012); S. F. King and C. Luhn, J. High Energy Phys. 03 (2012) 036; Y. Ahn, S. Baek, and P. Gondolo, Phys. Rev. D **86**, 053004 (2012); H. Ishimori and E. Ma, Phys. Rev. D **86**, 045030 (2012); E. Ma, A. Natale, and A. Rashed, Int. J. Mod. Phys. A **27**, 1250134 (2012); G. Branco, R. Gonzalez Felipe, F. Joaquim, and H. Serodio, Phys. Rev. D **86**, 076008 (2012); M.-C. Chen, J. Huang, J.-M. O'Bryan, A. M. Wijangco, and F. Yu, arXiv:1210.6982.

[31] S. King, Phys. Lett. B **659**, 244 (2008); W. Grimus and L. Lavoura, J. High Energy Phys. 09 (2008) 106; C. H. Albright and W. Rodejohann, Eur. Phys. J. C **62**, 599 (2009); S.-F. Ge, D. A. Dicus, and W. W. Repko, Phys. Lett. B **702**, 220 (2011); Phys. Rev. Lett. **108**, 041801 (2012); D. Hernandez and A. Y. Smirnov, Phys. Rev. D **86**, 053014 (2012); arXiv:1212.2149.

[32] M. Holthausen and M. A. Schmidt, J. High Energy Phys. 01 (2012) 126.

[33] K. Babu and S. Gabriel, Phys. Rev. D **82**, 073014 (2010).

[34] J. Beringer *et al.* (Particle Data Group), Phys. Rev. D **86**, 010001 (2012).

[35] N. Haba, A. Watanabe, and K. Yoshioka, Phys. Rev. Lett. **97**, 041601 (2006).

[36] X.-G. He and A. Zee, Phys. Lett. B **645**, 427 (2007).

[37] H. Ishimori, Y. Shimizu, M. Tanimoto, and A. Watanabe, Phys. Rev. D **83**, 033004 (2011).

[38] X.-G. He and A. Zee, Phys. Rev. D **84**, 053004 (2011).

[39] I. K. Cooper, S. F. King, and C. Luhn, J. High Energy Phys. 06 (2012) 130.

[40] F. Feruglio, C. Hagedorn, Y. Lin, and L. Merlo, Nucl. Phys. **B809**, 218 (2009).

[41] F. Borzumati and A. Masiero, Phys. Rev. Lett. **57**, 961 (1986).

[42] F. Feruglio, C. Hagedorn, Y. Lin, and L. Merlo, Nucl. Phys. **B832**, 251 (2010).

[43] E. Ma and M. Raidal, Phys. Rev. Lett. **87**, 011802 (2001).

[44] L. Lavoura, Eur. Phys. J. C **29**, 191 (2003).

[45] J. Adam *et al.*, Phys. Rev. Lett. **107**, 171801 (2011).

[46] G. Bennett *et al.*, Phys. Rev. D **73**, 072003 (2006).

[47] F. Jegerlehner and A. Nyffeler, Phys. Rep. **477**, 1 (2009).

[48] M. Hirsch, S. Morisi, E. Peinado, and J. Valle, Phys. Rev. D **82**, 116003 (2010); D. Meloni, S. Morisi, and E. Peinado, Phys. Lett. B **697**, 339 (2011); R. de Adelhart Toorop, F. Bazzocchi, and S. Morisi, Nucl. Phys. **B856**, 670 (2012); D. Meloni, S. Morisi, and E. Peinado, Phys. Lett. B **703**, 281 (2011); M. S. Boucenna, M. Hirsch, S. Morisi, E. Peinado, M. Taoso, and J. W. F. Valle, J. High Energy Phys. 05 (2011) 037; M. Boucenna, S. Morisi, E. Peinado, Y. Shimizu, and J. Valle, Phys. Rev. D **86**, 073008 (2012); L. Lavoura, S. Morisi, and J. Valle, arXiv:1205.3442.

[49] B. Grzadkowski, M. Iskrzynski, M. Misiak, and J. Rosiek, J. High Energy Phys. 10 (2010) 085.

[50] K. Ichiki, M. Oguri, and K. Takahashi, Phys. Rev. Lett. **93**, 071302 (2004).
[51] Y. Gong and X. Chen, Phys. Rev. D **77**, 103511 (2008).
[52] S. Palomares-Ruiz, Phys. Lett. B **665**, 50 (2008).
[53] M. Cirelli, P. Panci, and P. D. Serpico, Nucl. Phys. **B840**, 284 (2010).
[54] H. Davoudiasl, D. E. Morrissey, K. Sigurdson, and S. Tulin, Phys. Rev. D **84**, 096008 (2011).
[55] T. Hambye, F.-S. Ling, L. Lopez Honorez, and J. Rocher, J. High Energy Phys. 07 (2009) 090.
[56] K. Griest and D. Seckel, Phys. Rev. D **43**, 3191 (1991).
[57] S. Andreas, T. Hambye, and M. H. Tytgat, J. Cosmol. Astropart. Phys. 10 (2008) 034.
[58] E. Aprile *et al.*, Phys. Rev. Lett. **107**, 131302 (2011).
[59] K. Griest, Phys. Rev. D **38**, 2357 (1988).
[60] K. Griest, M. Kamionkowski, and M. S. Turner, Phys. Rev. D **41**, 3565 (1990).
[61] P. Frampton and T. Kephart, Int. J. Mod. Phys. A **10**, 4689 (1995); A. Aranda, C. D. Carone, and R. F. Lebed, Phys. Rev. D **62**, 016009 (2000); F. Feruglio, C. Hagedorn, Y. Lin, and L. Merlo, Nucl. Phys. **B775**, 120 (2007); P. H. Frampton and T. W. Kephart, J. High Energy Phys. 09 (2007) 110; P. H. Frampton, T. W. Kephart, and S. Matsuzaki, Phys. Rev. D **78**, 073004 (2008); D. A. Eby, P. H. Frampton, and S. Matsuzaki, Phys. Lett. B **671**, 386 (2009); D. A. Eby, P. H. Frampton, X.-G. He, and T. W. Kephart, Phys. Rev. D **84**, 037302 (2011).
[62] W. Grimus, L. Lavoura, O. Ogreid, and P. Osland, Nucl. Phys. **B801**, 81 (2008).
[63] J. Baglio, A. Djouadi, and R. Godbole, Phys. Lett. B **716**, 203 (2012).
[64] T. Plehn and M. Rauch, Europhys. Lett. **100**, 11002 (2012).
[65] CERN, Geneva, Technical Report ATLAS-CONF-2012-127, 2012.
[66] S. Chatrchyan *et al.* (CMS Collaboration), J. High Energy Phys. 07 (2012) 143.
[67] G. Aad *et al.* (ATLAS Collaboration), J. High Energy Phys. 06 (2012) 039.
[68] M. Carena, I. Low, and C. E. Wagner, J. High Energy Phys. 08 (2012) 060.
[69] S. Davidson and P. Verdier, Phys. Rev. D **86**, 111701 (2012).
[70] P. J. Fox, R. Harnik, J. Kopp, and Y. Tsai, Phys. Rev. D **84**, 014028 (2011).
[71] M. Holthausen, M. Lindner, and M. A. Schmidt, arXiv:1211.6953.